





Article

Energy and Techno-Economic Assessment of Cooling Methods on Blue Hydrogen Production Processes

William George Davies ¹, Shervan Babamohammadi ², Ilies Galloro ³, Mikhail Gorbounov ¹,
Francesco Coletti ^{1,4}, Monomita Nandy ⁵ and Salman Masoudi Soltani ^{1,*}

¹ Department of Chemical Engineering, Brunel University of London, Uxbridge UB8 3PH, UK; billy.davies@brunel.ac.uk (W.G.D.)

² Centre for Engineering Innovation and Research, School of Engineering, Computing and Mathematical Sciences, University of Wolverhampton, Wolverhampton WV1 1LZ, UK

³ Université Paul Sabatier Toulouse III, 31400 Toulouse, France

⁴ Hexxcell Ltd., Foundry Building, 77 Fulham Palace Road, London W6 2AF, UK

⁵ Brunel Business School, Brunel University of London, Uxbridge UB8 3PH, UK

* Correspondence: salman.masoudisoltani@brunel.ac.uk; Tel.: +44-(0)-1895-265884

Abstract

Blue hydrogen is a promising low-carbon alternative to conventional fossil fuels. This technology has been garnering increasing attention with many technological advances in recent years, with a particular focus on the deployed materials and process configurations aimed at minimising the cost and CO₂ emissions intensity of the process as well as maximising efficiency. However, less attention is given to the practical aspects of large-scale deployment, with the cooling requirements often being overlooked, especially across multiple locations. In particular, the literature tends to focus on CO₂ emissions intensity of blue hydrogen production processes, with other environmental impacts such as water and electrical consumption mostly considered an afterthought. Notably, there is a gap to understand the impact of cooling methods on such environmental metrics, especially with technologies at a lower technology readiness level. Herein, two cooling methods (namely, air-cooling versus water-cooling) have been assessed and cross-compared in terms of their energy impact alongside techno-economics, considering deployment across two specific locations (United Kingdom and Saudi Arabia). A sorption-enhanced steam-methane reforming (SE-SMR) coupled with chemical-looping combustion (CLC) was used as the base process. Deployment of this process in the UK yielded a levelised cost of hydrogen (LCOH) of GBP 2.94/kg H₂ with no significant difference between the prices when using air-cooling and water-cooling, despite the air-cooling approach having a higher electricity consumption. In Saudi Arabia, this process achieved a LCOH of GBP 0.70 and GBP 0.72 /kg H₂ when using air- and water-cooling, respectively, highlighting that in particularly arid regions, air-cooling is a viable approach despite its increased electrical consumption. Furthermore, based on the economic and process performance of the SE-SMR-CLC process, the policy mechanisms and financial incentives that can be implemented have been discussed to further highlight what is required from key stakeholders to ensure effective deployment of blue hydrogen production.

Keywords: blue hydrogen; carbon capture; technoeconomic analysis; air cooling; water cooling



Academic Editors: Fausto Gallucci, Orlando Palone, Gabriele Gagliardi and Serena Agnolin

Received: 7 July 2025

Revised: 31 July 2025

Accepted: 18 August 2025

Published: 20 August 2025

Citation: Davies, W.G.; Babamohammadi, S.; Galloro, I.; Gorbounov, M.; Coletti, F.; Nandy, M.; Soltani, S.M. Energy and Techno-Economic Assessment of Cooling Methods on Blue Hydrogen Production Processes. *Processes* **2025**, *13*, 2638. <https://doi.org/10.3390/pr13082638>

Copyright: © 2025 by the authors. Licensee MDPI, Basel, Switzerland. This article is an open access article distributed under the terms and conditions of the Creative Commons Attribution (CC BY) license (<https://creativecommons.org/licenses/by/4.0/>).

1. Introduction

Rising anthropogenic greenhouse gas (GHG) emissions, particularly CO₂, are major drivers of global warming, ecosystem degradation, and extreme weather events, underscoring the urgent need for decarbonisation. Hydrogen offers potential for reducing emissions in sectors such as transport, power, and heavy industry [1]. However, conventional production methods (grey hydrogen) like steam-methane reforming (SMR) emit significant CO₂, approximately 9 kg per kg of hydrogen produced [1,2]. Blue hydrogen, defined as hydrogen produced from fossil sources with carbon capture and storage (CCS), is a transitional technology bridging conventional grey hydrogen and green hydrogen from electrolysis. While this approach is commercially mature, it has efficiency penalties and cannot capture 100% of carbon (practical capture rates are typically 90–95%). Over the past decade, significant research has focused on advanced process configurations to improve the energy efficiency and carbon capture rate of blue hydrogen [3]. Two of the most advanced configurations for blue hydrogen are sorption-enhanced steam methane reforming (SE-SMR) and chemical-looping combustion (CLC), often used in tandem.

SE-SMR integrates a CO₂ sorbent (usually CaO) directly into the reforming reactor, enhancing hydrogen yield by shifting equilibrium reactions and enabling in situ carbon capture [2]. In effect, SE-SMR can operate auto-thermally, without the large furnace required in standard SMR, as the exothermic CO₂ sorption provides much of the needed heat internally [4]. SE-SMR has been shown to significantly increase hydrogen yield and purity while simultaneously capturing CO₂ from the reaction mixture. Laboratory and pilot studies over the last decade have validated the SE-SMR concept (current technology readiness level ~4–5) [5]. For example, the Gas Technology Institute demonstrated a pilot SE-SMR unit producing hydrogen at 71 kW_{th} scale with >80% H₂ purity [6].

The challenge in SE-SMR is that the CO₂ sorbent eventually becomes saturated and must be regenerated (releasing the CO₂) in a separate step. A key requirement for blue hydrogen is that the CO₂ released during regeneration be kept separate (concentrated CO₂ suitable for capture, not vented). Conventional regeneration by heating the sorbent with a combustion flue gas (from burning fuel in air) is not viable, because that would dilute the CO₂ with nitrogen [3]. Thus, various studies have explored regeneration via oxy-fuel combustion and, more recently, CLC [7,8].

In the oxy-fuel approach, fuel is combusted with pure O₂ (from an air separation unit (ASU)) to provide heat for regenerating the CO₂ sorbent, producing a concentrated CO₂ stream. Martínez et al. (2019) assessed an oxyfuel SE-SMR process in a hydrogen plant and achieved over 98% carbon capture with an equivalent hydrogen production efficiency of ~75% (lower heating value (LHV) basis) [9]. This high capture rate is because both sources of CO₂ (the reforming-produced CO₂ and the combustion CO₂ for heat) are captured: the former via the sorbent and the latter via the pure CO₂ from oxy-combustion. However, the need for an ASU imposes an energy and cost penalty. A study by Yan et al. (2020b) [10] noted that integrating oxy-fuel combustion for sorbent calcination reduced net efficiency by about 2.7 percentage points compared to other regeneration methods, due to the ASU power load.

The second (and increasingly favoured) approach is to integrate CLC with the SE-SMR process. In a CLC system, a solid oxygen carrier (typically a metal oxide like NiO or CuO) is used to transfer oxygen for combustion without direct contact between fuel and air [3,11]. The metal oxide is alternately oxidised by air in one reactor and reduced by the fuel (e.g., natural gas or reformer off-gas) in another, releasing heat. Importantly, the fuel in a CLC reduces the metal oxide and produces CO₂ and H₂O without nitrogen dilution, so a pure CO₂ stream can be obtained after condensing water [3,12].

Several studies have examined combining SE-SMR with a Ni-based CLC loop to supply the regeneration heat for the CO₂ sorbent [8,10–12]. In this configuration, the exothermic oxidation of Ni to NiO (in air) produces hot solids that are circulated to provide heat for the endothermic calcination of CaCO₃ (regenerating CaO and releasing CO₂), and the NiO is reduced by fuel in a separate step. Alam (2017) achieved a hydrogen production efficiency of 70.7% with 95.1% of carbon captured using a CLC-integrated SE-SMR process [12]. Later, Yan et al. (2020b) [10] evaluated multiple SE-SMR process configurations for blue H₂ at industrial scale, including cases with conventional heating, oxyfuel, and CLC. They showed that integrating SE-SMR with CLC and pressure swing adsorption (PSA) for H₂ purification could achieve nearly 100% CO₂ capture with a net efficiency up to 76.3%, markedly higher than a traditional SMR with CCS. This CLC-integrated design (SE-SMR + CLC + PSA) had the best performance of the six configurations studied by Yan et al., highlighting the efficacy of combining these technologies [10]. In a subsequent study, Yan et al. (2020a) [7] demonstrated that SE-SMR integrated with CLC could achieve over 95% CO₂ capture with competitive efficiencies and levelized hydrogen costs (LCOH) ranging between GBP 1.90–2.80 kg H₂.

Overall, the integration of SE-SMR and CLC is a major trend in blue hydrogen research, aiming to maximise carbon capture while minimising efficiency loss. By employing in situ CO₂ capture and using chemical looping to supply regeneration energy (instead of an external furnace), these systems virtually eliminate direct CO₂ emissions. Other process intensification strategies, including membrane-assisted separation and indirect heating methods, are further enhancing the appeal of SE-SMR. These configurations eliminate the need for externally fired heaters and shift the system toward near-zero emissions [13,14]. Additionally, applying high-performance CO₂ sorbents and cyclic reactors improves long-term process stability and scalability.

One crucial aspect of hydrogen production is water usage and environmental impact. Large-scale hydrogen production is energy-intensive, and substantial heat must be removed for safe and efficient operation. Traditionally, water-based cooling (via cooling water or evaporative cooling towers) is employed in SMR plants due to water's high heat capacity and the effectiveness of evaporative cooling. However, this comes at the cost of significant water consumption. Studies estimate that roughly 30% of the total water withdrawals associated with hydrogen production (SMR processes) are consumed by cooling systems [15]. In fact, adding CCS to SMR further increases cooling water requirements, since CCS (e.g., solvent scrubbing systems) introduce additional cooling and solvent regeneration needs [16].

Water-cooling systems, typically implemented as once-through, open-loop, or closed-loop evaporative systems, are valued for their compact design and high thermal conductivity. However, their significant water consumption poses challenges, especially in arid or drought-prone areas. For example, an SMR with CCS has been reported to consume about 32.2 L of water per kg H₂ produced (vs. ~30.4 L/kg without CCS), primarily due to extra cooling duties [16]. Arup (2022) [17] reported that a blue hydrogen facility employing water cooling could consume between 28 and 35 L of water per kg of hydrogen, depending on the process integration and CO₂ capture efficiency.

Air-cooled heat exchangers or dry cooling systems eliminate most process water consumption by using ambient air to carry away heat, albeit often with larger equipment and fan power requirements. In practice, there are trade-offs between water and air cooling. Evaporative (water) cooling is often more thermodynamically efficient and cost-effective than dry cooling for a given duty [18]. Ellersdorfer et al. (2025) [18] found that in large hydrogen electrolysis facilities, evaporative cooling systems could be up to 8× cheaper to implement than equivalent dry cooling systems for the same heat removal capacity.

The ability of water cooling to achieve lower temperatures (approaching the water's wet-bulb temperature) means smaller temperature differentials, and thus smaller required heat exchange area, explaining its lower cost in many cases [18]. Air cooling, by contrast, typically operates at higher minimum temperatures (limited by ambient air dry-bulb temperature) and often requires larger exchangers and fans, raising capital and operating costs [18]. Despite this, the advantage of air cooling is the drastic reduction in water use, a critical factor in arid regions or where water resources are constrained [16]. Recent analyses strongly encourage using "water-efficient cooling technologies such as air cooling" for hydrogen projects in water-scarce areas [19]. This is echoed by the International Renewable Energy Agency (IRENA), which notes that hydrogen projects in desert climates should minimise freshwater consumption by opting for dry cooling when feasible [19].

In summary, air versus water cooling presents a trade-off between water conservation and cost-effectiveness. Water cooling remains the predominant choice for most current hydrogen plants (including blue hydrogen from SMR) due to its lower cost and excellent heat rejection capability. Indeed, most literature studies on hydrogen production assume conventional water-cooling utilities (cooling towers or once-through water) as part of the plant design. For instance, an advanced blue hydrogen process study by Eluwah et al. (2023) assumed an external cooling water supply at 20 °C for condensing and heat recovery duties [20]. However, as sustainability concerns grow, researchers are increasingly recognising the need to evaluate dry cooling. The techno-economic impact of switching to air cooling can be significant: while it virtually eliminates process water consumption, it may slightly reduce overall plant efficiency (due to higher condensing temperatures) and increase costs. Some hydrogen production scenarios find that employing dry/air cooling would avoid approximately 6000–20,000 GL of water per year for a large future hydrogen facility (versus wet cooling), albeit with a moderate energy penalty [18]. Ultimately, the choice of cooling method in blue hydrogen production must balance water availability, environmental impact, energy efficiency, and economics. Emerging literature underscores that in regions with abundant water, traditional water cooling offers cost and efficiency benefits, whereas in water-limited areas, air cooling can be justified to ensure the water sustainability of hydrogen production [16].

Lin et al. (2025) assessed different hydrogen production technologies for water footprint of the process. They found that blue hydrogen production using amine scrubbing as the CCS method, consumed more water (~1.8 L/kg H₂) than a conventional SMR process [16]. Within the literature, there is a tendency to focus on technologies with a high readiness level such as amine scrubbing, especially when assessing further environmental metrics such as the water footprint. Lower technology readiness level (TRL) processes such as SE-SMR-CLC are often overlooked as they tend to focus on improved production efficiency [20]. Eluwah et al. (2023) developed an industrial SE-SMR process coupled with CLC, finding a high thermal efficiency of ~97.5% at a LCOH of USD 1.6/kg H₂ [20]. Whilst showing high efficiency and low cost, further exploration of the system is required.

Despite extensive research into integrating SE-SMR and CLC technologies for blue hydrogen production, the techno-economic implications of cooling strategies within these configurations remain underexplored. Most existing studies assume conventional water-based cooling without considering regional variations in water availability or the potential performance trade-offs associated with alternative methods such as dry (air) cooling. This oversight is particularly critical given that cooling systems not only significantly contribute to the overall water footprint of hydrogen production but also impact equipment sizing, land use, and operating efficiency (factors that can vary dramatically between temperate and arid climates). The current study addresses this gap by conducting a comprehensive comparative assessment of air versus water cooling in an SE-SMR-CLC

process for blue hydrogen production, by further focusing on two climatically distinct regions (i.e., UK and Saudi Arabia). This research evaluates how location-dependent parameters influence the selection and performance of the cooling methods. These scenarios are systematically analysed (water and air cooling in each location), concentrating on energy demand, heat exchanger sizing, land requirements, and cost implications. Additionally, a detailed sensitivity analysis of operational expenditure is undertaken to better understand the economic trade-offs and robustness of each configuration. Through this approach, the study aims to provide critical insights into how cooling infrastructure decisions affect the scalability and sustainability of next-generation blue hydrogen systems, ultimately supporting more location-sensitive and resource-aware deployment strategies, for early-TRL blue hydrogen production processes.

2. Research Methodology

2.1. Process Description and Scenarios Considered

The process assessed in this work is a sorption-enhanced steam methane reforming with chemical-looping combustion (SE-SMR-CLC), which has a production capacity of 432 tonnes of hydrogen per day, validated and developed in our previous work [21]. Figure 1 presents a block-flow diagram of the process. The steady-state simulation was developed in ASPEN Plus (V 12.1), with Peng-Robinson Boston-Mathias (PR-BM) property package used as the thermodynamic model [22]. The PR-BM was selected as it is commonly used to predict the behaviour of light hydrocarbons at high pressures, a key advantage when modelling an SE-SMR process [21].

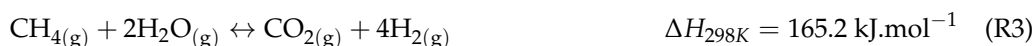
The reformer, calciner, air reactor (AR), and fuel reactor (FR) are modelled using the RGIBBS block. Natural gas (NG) and water are compressed and pressurised respectively to 25 bara and heated to 600 °C before entering the reformer with the CaO, where Reactions (R1)–(R4) occur. The solid and syngas are separated, with CaCO₃ moving into the calciner, where the reverse of (R4) takes place; CaO is recycled while the CO₂ stream is released. The gas then flows into a condenser, which cools the stream, allowing H₂O(l) to be condensed out. Subsequently, the syngas passes into a PSA. The hydrogen recovery is calculated by Equation (1) below. The hydrogen exits the column to be compressed by a three-stage compressor to 350 bara before being stored.

The PSA off-gas is recycled and mixed with NG, then heated to 600 °C prior to entering the FR at 1000 °C, where Reactions (R5)–(R7) occur. The reduced iron oxide is recycled for use in the AR at 1000 °C, where an air stream is heated and introduced into the AR, where R8 occurs. The oxygen-depleted air is cooled before leaving the system. The CO₂ from the calciner and the gas stream from the fuel reactor are mixed, cooled, and the liquid H₂O is condensed out to ensure a purer stream of CO₂ exits the system. The CO₂ is then compressed using a multi-stage compressor.

As mentioned earlier, the process is modelled as a steady-state simulation with certain assumptions (standard in early-stage modelling to reduce complexity while capturing key thermodynamic behaviour). These include: Steady-state operation, negligible pressure drop, and uniform temperature. These are reasonable assumptions given the design intent of well-insulated, efficiently mixed industrial reactors and allow for effective evaluation of process performance within acceptable accuracy limits. There are some limitations of utilising a steady-state approach. For example, sorbent performance degradation cannot be meaningfully captured by a steady-state process, as well as impacts within the cooling system such as the dynamic impact of fouling and transient effects in cooling towers. Nevertheless, in calculations of the variable operating costs, the performance degradation

of the sorbent has been factored in, as well as the fouling effects through incorporating fouling coefficients when sizing the heat exchangers.

$$H_2 \text{ Recovery in PSA (\%)} = 100 - \frac{100}{0.2521 \left(\frac{p_1}{p_2} \right) + 1.2706} \quad (1)$$



Within this work, four scenarios were considered. Air and water cooling were selected as the cooling methods; this is due to their abundant use in an industrial setting [18]. For each cooling method, two locations were selected: one is Swansea in the UK and the other is Neom in Saudi Arabia. These locations were chosen due to both countries developing hydrogen economies and their respective climates [19]. To assess the efficiency of the process, the following key performance indicators (KPIs) were considered: cold gas efficiency (CGE), net process efficiency (NPE), total process efficiencies (TPE), total electrical consumption (TEC) and CO₂ capture efficiency (CCE), these are calculated through Equations (2)–(6) respectively. These KPIs are to provide metrics to evaluate this process against other hydrogen production processes as well as considering the utilities that are used within this process.

$$CGE (\%) = \frac{m_{H_2} \times LHV_{H_2}}{m_{NG} \times LHV_{NG}} \times 100 \quad (2)$$

$$NPE (\%) = \frac{m_{H_2} \times LHV_{H_2}}{(m_{NG} \times LHV_{NG}) + \frac{P_e}{\eta_{e,eff}}} \times 100 \quad (3)$$

$$TPE (\%) = \frac{m_{H_2} \times LHV_{H_2}}{(m_{NG, total} \times LHV_{NG}) + \frac{P_e + P_u}{\eta_{e,eff}}} \times 100 \quad (4)$$

$$TEC (MW) = \sum P_e + P_u \quad (5)$$

$$CCE (\%) = \frac{m_{CO_2, out}}{m_{CO_2, total}} \times 100 \quad (6)$$

where m_{H_2} is the mass flow rate of hydrogen (kg/sec) leaving the system; LHV_{H_2} is the lower heating value of hydrogen (120 MJ/kg); m_{NG} is the mass flow rate of NG entering the fuel reactor and the reformer, with LHV_{NG} being the lower heating value of NG (47.1 MJ/kg); P_e is the electric work introduced to the system; $\eta_{e,eff}$ is the NG to electric energy conversion efficiency (49%); $m_{NG, total}$ is the mass flow rate of NG entering the steam generator, fuel reactor, and reformer; P_u is the electrical work from the utilities; and $m_{CO_2, out}$ is the CO₂ leaving the system to be stored while $m_{CO_2, total}$ is the total CO₂ leaving the system.

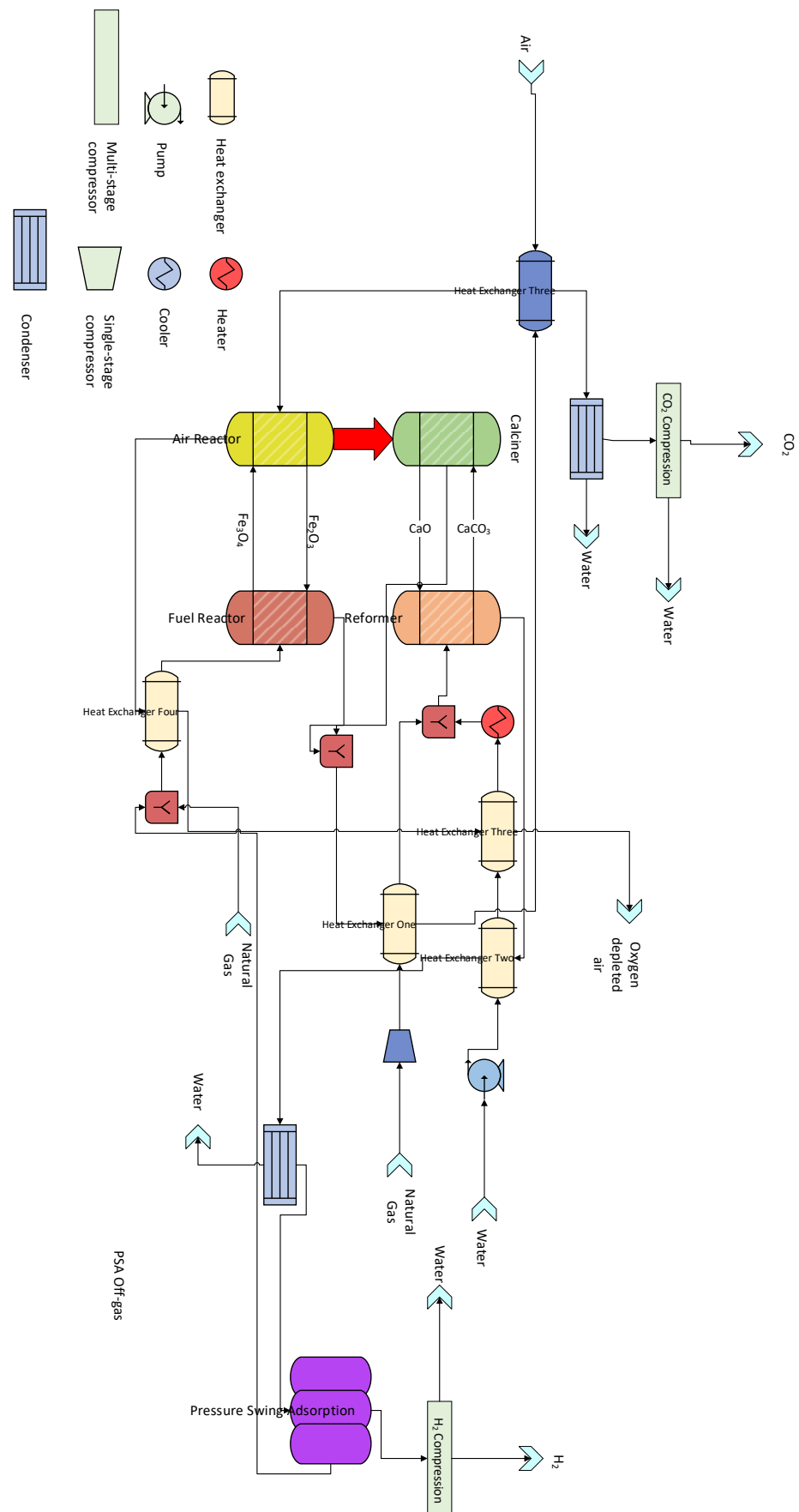


Figure 1. Process-flow diagram of sorption-enhanced steam methane reforming with chemical-looping combustion.

2.2. Calculations of Cooling Requirements and Design Assumptions of Cooling System/Scenario

Water cooling utilises water to cool the process stream through a conventional shell-and-tube heat exchanger, as illustrated in Figure 2a, whereas air cooling employs air to cool the process stream using a conventional finned-tube heat exchanger depicted in Figure 2b. For this blue hydrogen production process, following the pinch analysis conducted in previous work [21]. Cooling is required primarily for the knock-out drums preceding the PSA unit (hydrogen stream) and the multi-stage condenser (CO₂ stream), for each stage of compression in both the hydrogen and CO₂ streams, and for the oxygen-depleted air exiting the air reactor. The configuration of the water-cooling system of this system is shown in Figure 3, for the air-cooling it is a once through system. The heat duty for the condensers was determined via Equation (7), while the heat duty for the multi-stage compressor was determined via Equation (8). These equations are rearranged to calculate the mass flow rate of water and air required to cool the stream.

$$Q_{\text{cnd/cool}} = m_{\text{FR}} \times C_p \times \Delta T \quad (7)$$

$$Q_{\text{cmp}} = n \times m_{\text{FR}} \times C_p \times T_{\text{cnd}} \times \left[1 - \left(\frac{P_{\text{cmpout}}}{P_{\text{cmpin}}} \right)^{\frac{k-1}{n+k}} \right] \quad (8)$$

where m_{FR} represents the mass flow rate of water or air in kg/sec, Q_{cnd} and Q_{cool} denote the condenser heat duty and the cooler duty in kW, respectively, c_p is the heat capacity of water (4.17 kJ/kg°C) or air (1.007 kJ/kg°C), and ΔT is the change in temperature of the cooling water or air. Q_{cmp} is the heat duty of the compressor, n indicates the number of stages, T_{cnd} is the temperature of the inter-stage cooler, p_{cmpout} is the pressure of the compressor at the outlet, and p_{cmpin} is the pressure of the compressor at the inlet, with k being 1.803. To determine the size of the heat exchange area, Equation (9) is employed.

$$A = \frac{Q}{U \times \Delta T_{\text{lm}}} \quad (9)$$

where A is the heat transfer area in m²; in this work, a 25% area margin has been used thus the actual size of the heat exchanger is 1.25 times larger than A . This was selected as the design margin to account for uncertainties within the design and potential performance degradations within the heat exchanger. U , the heat transfer coefficient, is calculated using Equation (10) for water cooling, while Equation (11) is used for air cooling. ΔT_{lm} is calculated by Equation (12).

$$\frac{1}{U} = \frac{1}{h_i} + \frac{1}{h_0} + \frac{R_{f,i}}{A_i} + \frac{R_{\text{wall}}}{A_{\text{lm}}} + \frac{R_{f,0}}{A_o} \times \frac{A_i}{A_o} \quad (10)$$

$$\frac{1}{U} = \frac{1}{h_0 \eta_0} + \frac{1}{h_i} + \frac{R_{f,i}}{A_i} + \frac{R_{\text{wall}}}{A_{\text{lm}}} + \frac{R_{f,0}}{A_o} \times \frac{A_i}{A_o} \quad (11)$$

$$\Delta T_{\text{lm}} = \frac{(T1 - t2) - (T2 - t1)}{\ln \left(\frac{(T1 - t2)}{(T2 - t1)} \right)} \quad (12)$$

where h_i , h_0 are the inside and outside heat transfer coefficients; $R_{f,i}$, $R_{f,0}$ are the fouling resistance on the inside and outside of the tubes; A_i , A_o are the inside and outside surface areas, with the R_{wall} being the wall resistance; A_{lm} is the log-mean area; η_0 is the overall surface efficiency; $T1$ is the inlet tube side fluid/gas temperature; $t2$ is the outlet shell side liquid/gas temperature; $t1$ is the inlet shell side fluid/gas temperature; and $T2$ is the outlet tube side fluid/gas temperature. Further calculations for the heat exchanger design are provided in the Supplementary Information.

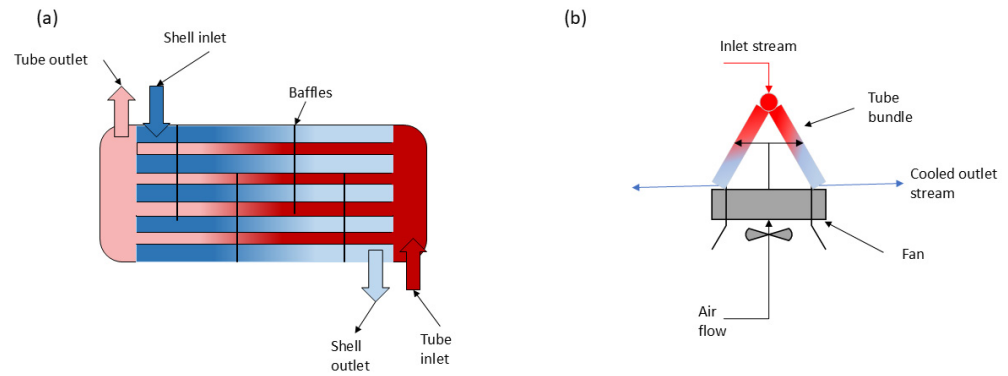


Figure 2. (a) Diagram of shell and tube heat exchanger for water cooling. (b) Diagram of a forced convection heat exchanger for air cooling.

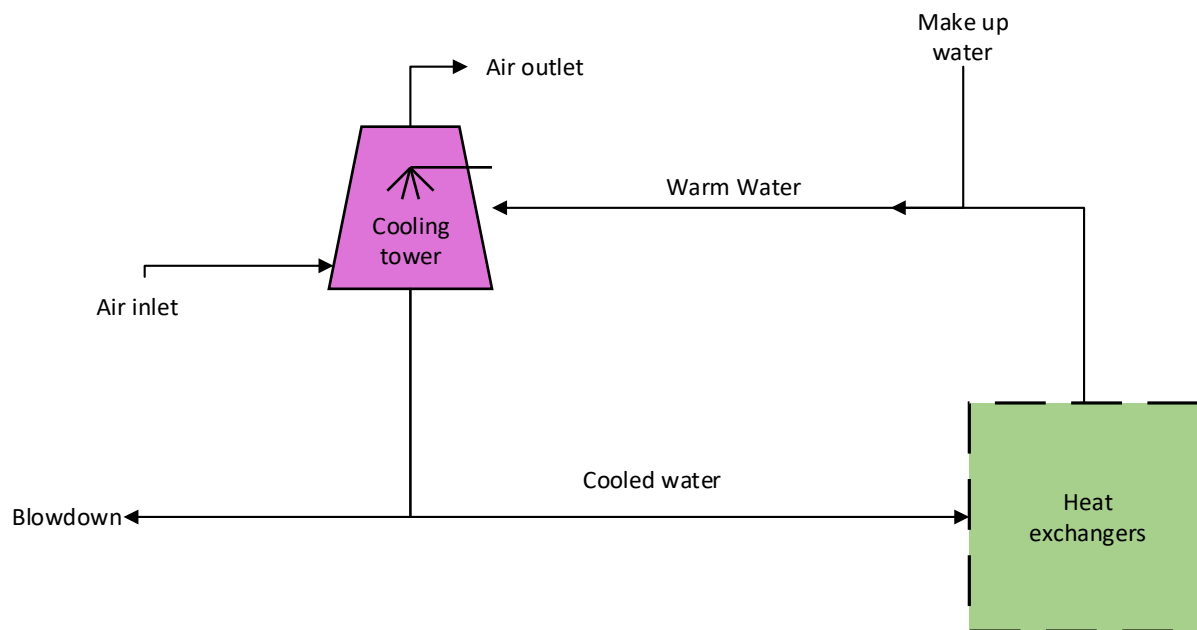


Figure 3. Basic flow diagram of water-cooling scenarios.

Table 1 highlights the selected temperature ranges for the cooling medium in each scenario. This is based on the wet-bulb temperature for each location for water cooling, while for air cooling, the dry-bulb temperature is considered. For each location, it is ensured that the temperature approach does not fall below 5 °C for both water cooling and air cooling.

Table 1. Temperature ranges for each scenario and selected cooling temperatures for the process.

	Scenario 1: Water-Cooling UK	Scenario 2: Air-Cooling UK	Scenario 3: Water-Cooling Saudi Arabia	Scenario 4: Air-Cooling Saudi Arabia
Inlet Cooling Stream Temperature	20	30	25	45
Outlet Cooling Stream Temperature	30	40	35	55
Approach temperature	5	15	5	15
Wet Bulb Temp Range (°C)	4–14	4–14	10–20	10–20
Dry Bulb Temp (°C)	6–16	6–16	17–35	17–35

For water-cooling Equation (13) is used to calculate the pump power and for air-cooling Equation (14) is used to calculate the fan power.

$$P_p = \frac{m_{FR} \times H \times SG}{\mu_{ps}} \quad (13)$$

$$P_f = \frac{dp \times q}{\mu_f \mu_b \mu_m} \quad (14)$$

where P_p is the power of the pump, m_{FR} is the mass flow rate of water in kg/sec, H is the dynamic head of the pump (metres), SG is the standard acceleration due to gravity at 9.81 m/s^2 , and μ_{ps} is the pump efficiency (75% is considered in this work). P_f is the fan power, dp is the pressure drop, q is the volumetric flow rate of air, μ_f is the fan efficiency (95%), μ_b is the belt efficiency (92%), and μ_m is the motor efficiency (90%). To evaluate cooling performance in each scenario, the following metrics are used: the average size of the heat exchanger (Equation (15)), the cooling demand (Equation (16)), the water consumption by cooling processes per kg of hydrogen produced (Equation (17)), and the electricity consumption for each scenario (Equation (5)).

$$A_{HX} = \frac{\sum s_{HX}}{n_{HX}} \quad (15)$$

$$CD_n = \sum Q_c \quad (16)$$

$$WC = \frac{\sum m_{H_2O}}{m_{H_2}} \quad (17)$$

Design of Cooling Tower for Each Location for Water-Based Cooling

Within this work, a cooling tower is used for the water-based cooling scenarios. A once-through system may be utilised but is typically selected when there is a substantial water source [23]. A cooling tower utilises air to cool the hot water entering through an evaporative process, employing a mechanically forced draft design. The cooling tower's design is dependent on location, with the minimum temperature to which the water can be cooled determined by the location's wet-bulb temperature [23]. Manufacturers can guarantee a 2.8°C approach to the wet-bulb temperature [23]. Design considerations for each location are illustrated in Table 2.

Table 2. Design considerations for each location for the cooling tower.

Design Considerations	UK	Saudi Arabia
Wet-bulb temperature ($^\circ\text{C}$)	4–14	10–20
Type of tower	Mechanical forced draft	Mechanical forced draft
Approach temperature ($^\circ\text{C}$)	5	5
Range Temperature	10	10
Cycles of Concentration (COC)	5	3

To calculate the mass flow rate of water being cooled by the cooling tower, Equation (18) is employed, which sums the streams entering the cooling tower. The evaporation rate is determined by Equation (19), the blowdown rate is determined by Equation (20), with the total top-up rate calculated by Equation (21), and the area of the cooling tower is calculated by Equation (22). The fan power needed for the cooling tower is calculated using Equation (14).

$$m_{\text{Total } H_2O} = \sum m_{FR} \quad (18)$$

$$\text{Evaporation rate} = 0.0018 \times m_{\text{Total H}_2\text{O}} \times \Delta T \quad (19)$$

$$\text{Blowdown rate} = \frac{\text{Evaporation rate}}{\text{COC} - 1} \quad (20)$$

$$\text{make up rate} = \text{Blowdown rate} + \text{Evaporation rate} \quad (21)$$

$$A_{CT} = \frac{m_{\text{Total H}_2\text{O}}}{\text{water holdup}} \times F \quad (22)$$

where $m_{\text{Total H}_2\text{O}}$ is the total mass flow rate of water required to cool down the system, ΔT is the approach temperature, and COC is the cycles of concentration. The water holdup for a mechanical forced draft cooling tower at $2.3 \text{ kgs}^{-1}\text{m}^{-2}$ and F is the fill factor, determined to be 0.57.

2.3. Techno-Economic Assessment Methodology

The techno-economic assessment was conducted based on the global CCS institute [24]. For each scenario, the process was evaluated using the LCOH as well as the cost of carbon avoided (COCA), which are calculated using Equations (23) and (24), respectively. The COCA provides a value for the minimum CO_2 emissions tax required to render this process more economically attractive in comparison to a conventional SMR plant. Each term in the LCOH is detailed in Table 3. The fixed charged factor (FCF) is calculated using Equation (25), converting the total capital value into uniform annual amounts, with a discount rate of 10% considered over a plant lifetime of 30 years.

$$\text{LCOH} = \frac{(\text{CAPEX}) \times (\text{FCF}) + \text{FOM}}{m_{\text{H}_2} \times (\text{CF} \times 8766)} + \text{VOM} + \text{FC} \times \text{HR} \quad (23)$$

$$\text{COCA} = \frac{\text{LCOH}_{\text{blueH}_2} - \text{LCOH}_{\text{greyH}_2}}{\left(\frac{m_{\text{CO}_2}}{m_{\text{H}_2}}\right)_{\text{greyH}_2} - \left(\frac{m_{\text{CO}_2}}{m_{\text{H}_2}}\right)_{\text{blueH}_2}} \quad (24)$$

$$\text{FCF} = \frac{r(1+r)^T}{(1+r)^T - 1} \quad (25)$$

Table 3. Definitions of factors in LCOH.

Parameter for LCOH Calculation	Definition	Unit
TCR	Total capital requirement	GBP
FCF	Fixed-charge factor	
FOM	Fixed operational costs	GBP/year
M_{H_2}	Mass of hydrogen produced	kg/hr
CF	Capacity factor	0.7 for year one 0.95 for year 2–30
VOM	Variable operational costs	GBP/year
HR	Net heat rate of plant	kWh/kg- H_2
FC	Fuel cost per unit of energy	GBP/kWh
r	Discount rate (assumed to be 10%)	
T	Economic lifetime of the plant (30 years)	years

Estimating the total capital requirement (TCR) for the process is done using the method described in Table 4, which uses the bare erected cost (BEC), which totals the installed cost of equipment. To calculate the BEC, Equation (26) was used. The costs have been adjusted for the year 2025 using Chemical Engineering Plant Cost Index (CEPCI) factors. The reference

values used to calculate the BEC is provided in the Supplementary Information. Given that the process involves technologies with a low technology readiness level (TRL), a process contingency of 30% was included, along with a project contingency of 10% [25]. Owner costs, including land, financing costs, inventory capital, and start-up costs, constitute approximately 20.2% of the total plant cost (TPC). A location factor was incorporated into the TCR cost. A factor of 1.14 is applied to calculate the total capital requirement, accounting for an increase in capital due to both escalation and interest during the construction of an investor-owned utility [26].

$$BEC = \sum C_A = \sum C_b \times \left(\frac{CI_A}{CI_B} \right) \times \left(\frac{S_A}{S_B} \right)^\alpha \quad (26)$$

where C_A is the cost of the equipment within this work and C_b is the cost of the original equipment. CI_A is the CEPCI factor in the year of the proposed design, with CI_B is the CEPCI factor of the year the original equipment was built. S_A is the capacity of the new equipment and S_B is the capacity of the original equipment with α of 0.6.

Table 4. Methodology and assumptions to estimate total capital requirement.

Component	Definition
Bare erected cost (BEC)	Sum of installed cost of equipment
Engineering Procurement Construction Cost (EPCC)	8% of BEC
Process contingency	30% for the sorption-enhanced reformer, fuel reactor and air reactor, 0% for the remaining units
Project contingencies	10% of (BEC, EPCC, and process contingencies)
Total contingencies	Project contingencies + process contingencies
Total plant cost (TPC)	BEC + EPCC + total contingencies
Location factor	1.05% \times PC for UK, 1.00 \times TPC for Saudi Arabia
Owners costs	20.2% of TPC
Total overnight cost	Location factor + owners cost
Total capital requirement	1.14 \times TOC

The operational expenditure (OPEX) is divided into fixed operating costs (FOM) and variable operating costs (VOM). The assumptions for the FOM and VOM are presented in Table 5. Due to the various scenarios considered, a sensitivity analysis was performed on natural gas prices, water costs, and electricity prices for each scenario (location dependent). The conversion rates are 0.20 for GBP to SAR, 0.85 for EUR to GBP, and 0.78 for USD to GBP. A lifespan of 500 h is considered for CaO, while a lifespan of 1000 h is deemed appropriate for iron oxide. For the nickel catalyst, activated carbon, and zeolite, a lifespan of five years is considered.

Table 5. Fixed and variable operating costs.

	Value		Unit	Reference
	Saudi Arabia	United Kingdom		
Fixed Operational Costs				
Operating Labour	30,000	30,000	GBP	[27,28]

Table 5. *Cont.*

	Value		Unit	Reference
Number of Workers	45 (15 per 8-h shift)	45 (15 per 8-h shift)		
Maintenance, Support and Administrative Labour	2.5	2.5	% of TOC	
Insurance and Property Taxes	2	2	% of TOC	
NG Prices	0.001	0.10	GBP/kWh	[29,30]
Variable Operational Costs				
Cooling Water	1	0.5	GBP/m ³	[31,32]
Process Water	5.50	3	GBP/m ³	[31,32]
Oxygen Carrier (Iron Oxide)	6	6	GBP/kg	[33]
Calcium Oxide	0.85	0.85	GBP/kg	[34]
Nickel Catalyst	25	25	GBP/kg	[35]
Activated Carbon	1.10	1.10	GBP/kg	[36]
Zeolite	1.50	1.50	GBP/kg	[37]
Electricity Cost	0.03	0.20	GBP/kWh	[29,38]
CO ₂ Storage and Transportation Costs	20	28	GBP/tonneCO ₂	[39]
Emission Tax	0	18	GBP/tonne	[40]

3. Results and Discussions

3.1. Process Performance

The KPIs for the SE-SMR-CLC process are shown in Table 6 without considering any utility values within the calculation; this highlights the technical performance of the process, demonstrating it to be a highly efficient method of producing hydrogen while simultaneously capturing CO₂.

Table 6. KPIs for SE-SMR-CLC system developed.

	CGE (%)	NPE (%)	CCE (%)
SE-SMR-CLC	87.52	73.86	99.58

A further evaluation of the process KPIs was considered for each scenario, including the impact of the utilities. For example, electricity consumption from utility units such as air-cooling was considered, as well as the natural gas (NG) used for the steam generator to calculate the CCE and TPE; the results are shown in Table 7.

Table 7. KPI for process across each scenario including utilities consumption.

	TPE (%)	CCE (%)	LCOH (GBP/kg H ₂)	Electricity Consumption (MW)
UK, water cooling	62.36	92.95	2.94	73.18
UK, air cooling	62.15	92.95	2.94	74.83
Saudi Arabia, water cooling	62.33	92.95	0.72	72.72
Saudi Arabia, air cooling	61.64	92.95	0.70	78.07

The initial assessment of the process demonstrates an efficient method for producing hydrogen on a larger scale whilst capturing CO₂. Using NG for the steam generator (SG) yields a CCE of 92.95%. In contrast, utilising an electric SG can achieve a higher total CCE (99.01%), but comes with significantly higher electrical consumption (over 100 MW), leading to a lower total process efficiency (if utilities are considered) and a higher LCOH, for example if an electric SG were used the LCOH within the UK scenarios increases by GBP 0.30 /kg H₂ and the Saudi Arabia scenarios the LCOH increases by GBP 0.08/kg H₂. Consequently, the NG SG was considered for future implementation. Across each scenario, there are slight differences in NPE due to the variation in electrical consumption among the processes. Figure 4 illustrates the breakdown of electrical consumption in each scenario.

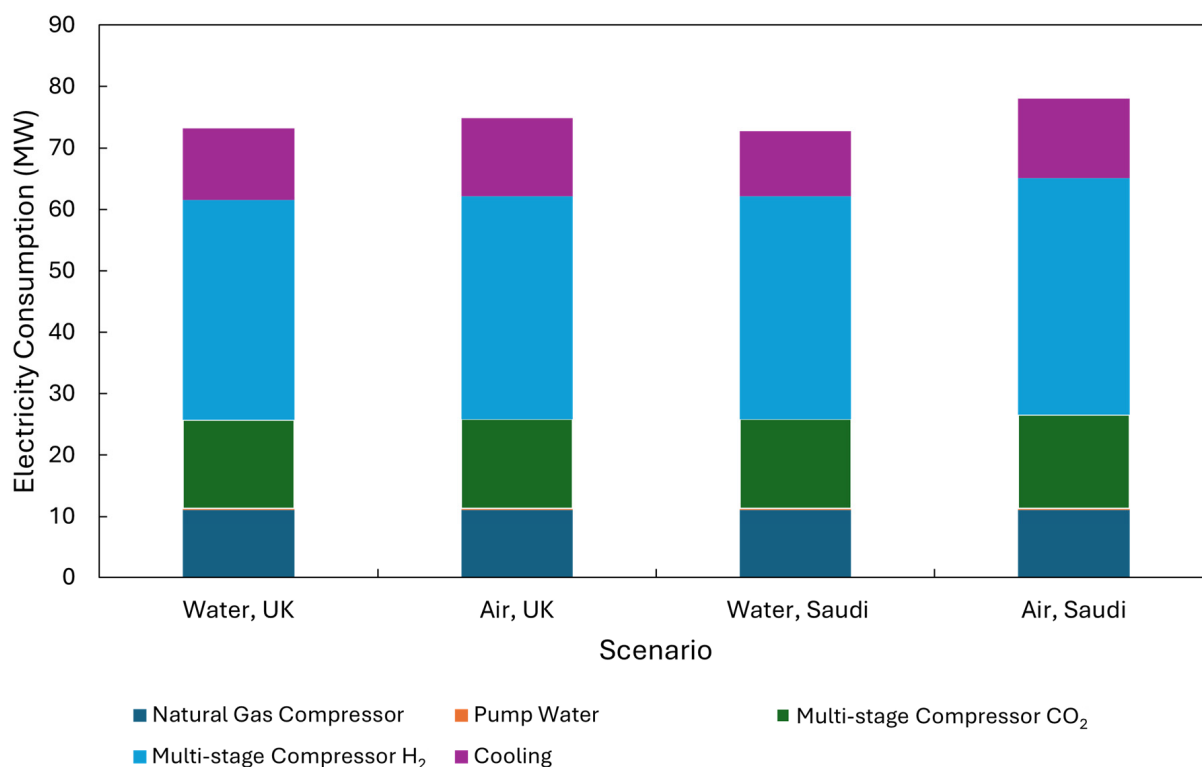


Figure 4. Breakdown of electricity consumption for each unit within each scenario.

As illustrated in Figure 4, most electrical consumption originates from the use of multi-stage compressors, which account for over 50 MW across all scenarios. The hydrogen compressor is the most significant contributor, responsible for 35–38 MW (depending on the scenario) of electrical consumption. The Saudi Arabia air scenario appears to exhibit the highest electrical consumption. This is due to the air-cooling method employed for cooling the streams, which cools the gas between stages to a higher temperature than would be achieved with water cooling. The elevated temperature at which the gas enters the compressor's stage requires more effort to compress the gas. Both air-cooling scenarios demonstrate greater electrical consumption than the water-cooling scenarios due to the increased workload on the compressors, as well as the heightened electrical consumption for cooling stemming from the fan power required for the air-cooling streams.

3.2. Assessment of Cooling System

3.2.1. Cooling Requirements

Figure 5 illustrates the cooling requirements for each scenario. As shown, the UK scenarios for both air and water cooling demonstrate a higher cooling requirement; this is due to the colder climate in the UK, which allows the streams to be cooled to a lower

temperature. The primary unit operator across these approaches is the H₂ condenser, accounting for approximately 65% of the total cooling requirement in each scenario. This is because a phase change occurs within this unit at high pressure, necessitating a significant cooling requirement to ensure that the desired temperature is achieved.

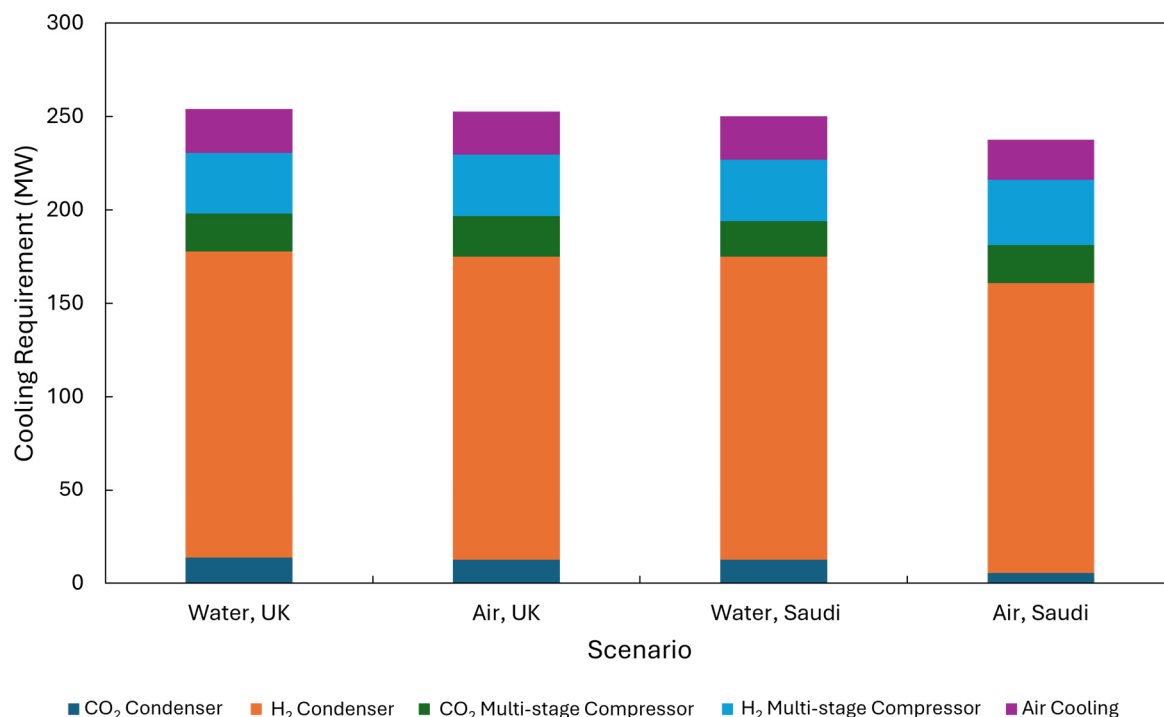


Figure 5. Cooling demand within each scenario.

Capturing CO₂ requires an additional cooling capacity of 25–31 MW (depending on the scenario) due to the CO₂ condenser and multi-stage compressor, contributing between 10% and 13% to the overall cooling requirement of the system. Compared to conventional CO₂ capture technologies, this method offers distinct advantages; for instance, Brandl et al. (2017) found that employing amine absorption technology in a post-combustion CO₂ plant increases the cooling load by up to 47% for a subcritical plant [41]. The combination of in situ capture technologies with the heat exchanger network (HEN) used in this process minimises the cooling impact on the operation. The primary concern regarding air cooling is its efficiency; the lower heat capacity of air results in a diminished heat transfer coefficient, necessitating a higher mass flow rate of air to cool the stream, which in turn raises the electrical consumption of the plant. Together, these factors increase the overall cost of the plant, as the reduced heat capacity demands a larger heat exchange area to cool the stream effectively. Table 8 provides an overview of the cooling KPIs for each scenario.

Table 8. KPIs for cooling units across each scenario.

Scenarios	Average Heat Exchanger Size (m ²)	Cooling Demand (MW)	Electrical Consumption of Cooling (MW)	Water Consumption of Whole Process (Cooling Units) (L/kg H ₂)
Water, UK	1567.625	230.44	11.67	42.50 (27.26)
Air, UK	3432.33.80	229.48	12.66	15.24 (0)
Saudi Arabia, Water	1576.54	226.82	10.54	44.82 (29.58)
Saudi Arabia, Air	3097.26.	216.11	12.94	15.24 (0)

As shown in the air scenario, a significantly larger heat exchanger area is needed to cool these streams. Despite a slightly lower cooling demand, the electrical consumption is slightly higher. Although not as significant due to the cooling tower being a mechanical forced draft. This will result in potentially higher costs for both the TCR (heat exchanger sizing) and VOM (electrical consumption). Additionally, the increased water consumption may also lead to a higher VOM, depending on water costs, which will have a particularly significant impact in arid regions like Saudi Arabia. This will be discussed in greater detail in Section 3.3.

3.2.2. Cooling Tower

The cooling tower for each water-cooling scenario had total cooling requirements of 256.92 MW and 232.23 MW for the UK and Saudi Arabia scenarios, respectively. The lower cooling demand in Saudi Arabia is attributed to the warmer climate. However, due to the location, the efficiency of the cooling is reduced, which results in higher bleed-off within the system. This necessitates a higher water top-up, increasing the water consumption. Table 9 provides a breakdown of the cooling towers performance in each location.

Table 9. Performance of cooling tower across each location.

	UK	Saudi Arabia
Mass flow rate of water entering (kg/sec)	6161.32	5569.58
Evaporation rate (kg/sec)	110.90	100.25
Bleed off rate (kg/sec)	27.73	50.13
Size of cooling tower (m ²)	1526.94	1380.29

3.2.3. Water Consumption: Impact of Cooling System

When utilising water-based cooling methods, it is also essential to evaluate water consumption; Figure 6 illustrates the comparison across various scenarios. As shown in Figure 6, there is an increase in water consumption when employing evaporative cooling. Among the two water-cooling approaches, the UK exhibits slightly lower water consumption. This is attributable to the improved efficiency of the cooling tower, indicating that the water losses from the cooling tower are less than those in Saudi Arabia.

In comparison to other systems, the water-cooling approaches demonstrate higher water consumption than alternative technologies, as indicated in Table 10. This is attributed to the high S/C ratio selected; a ratio of five results in an increased cooling requirement to lower the temperature of the stream exiting the reformer. Due to the CO₂ capture technologies chosen, there is no increase in water consumed by the process; the extra water consumption is attributed to the cooling of each stream. A breakdown of the water consumption by each cooling stream is illustrated in Figure 7a,b.

As shown in Figure 7a,b, the H₂ condenser exhibits the highest water consumption for cooling, necessitating 17.42 and 20.69 L/kg H₂ for the UK and Saudi Arabia, respectively. This is again attributed to the substantial volumes of steam condensed from the hydrogen stream exiting the reformer. The condenser and multi-stage compressor for the CO₂ stream account for 3.90 and 4.34 L/kg H₂ in the UK and Saudi Arabia scenarios, respectively. In comparison to the literature, the SE-SMR coupled with CLC shows promise, especially when using air-cooling, the water consumption is significantly reduced across both scenarios as shown in Table 10: a reduction of water consumption by up to 55% in comparison to the SE-SMR coupled with CLC. As expected, when utilising water-cooling, the water consumption within the SE-SMR-CLC is increased in comparison to other blue-hydrogen production processes.

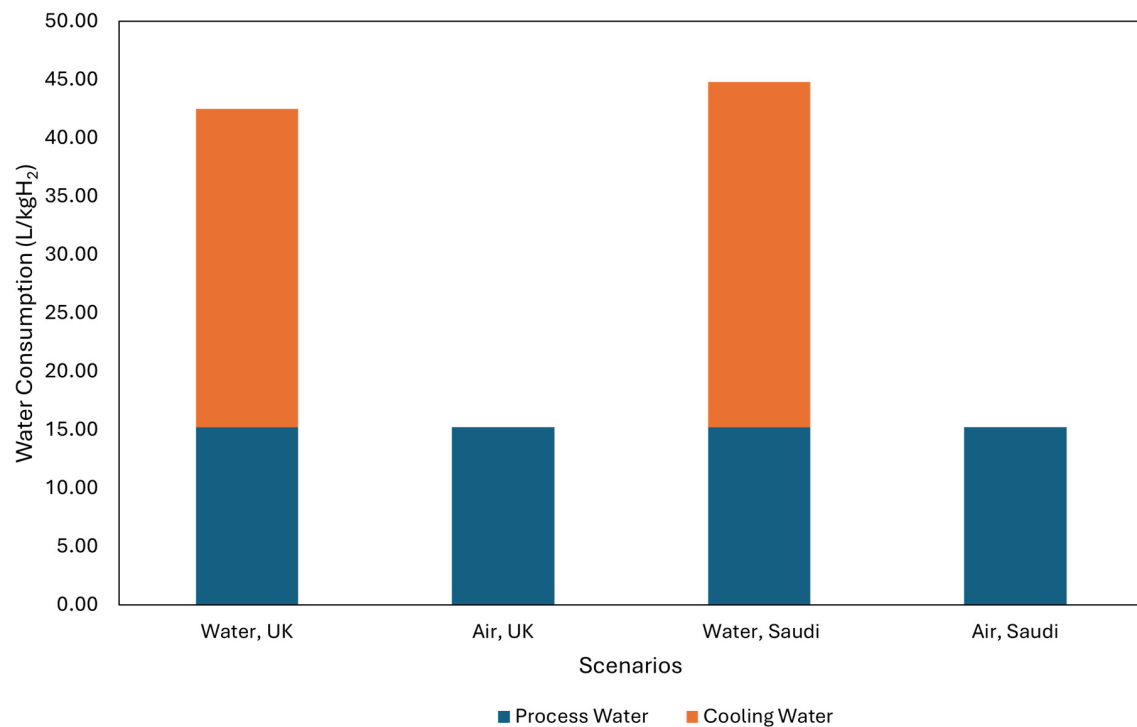


Figure 6. Water consumption across each scenario.

Table 10. Treated water demand for hydrogen production.

Process Configuration	Water Consumption (L/kg H ₂)
SMR (No CCS) [17]	27.8
SMR + 90% CCS [17]	32.2
SE-SMR + Oxy-fuel [17]	33.5
SE-SMR + CLC, air cooling (This work)	15.4
SE-SMR+CLC, UK water (This work)	42.50
SE-SMR + CLC, Saudi Arabia, water (This work)	44.82

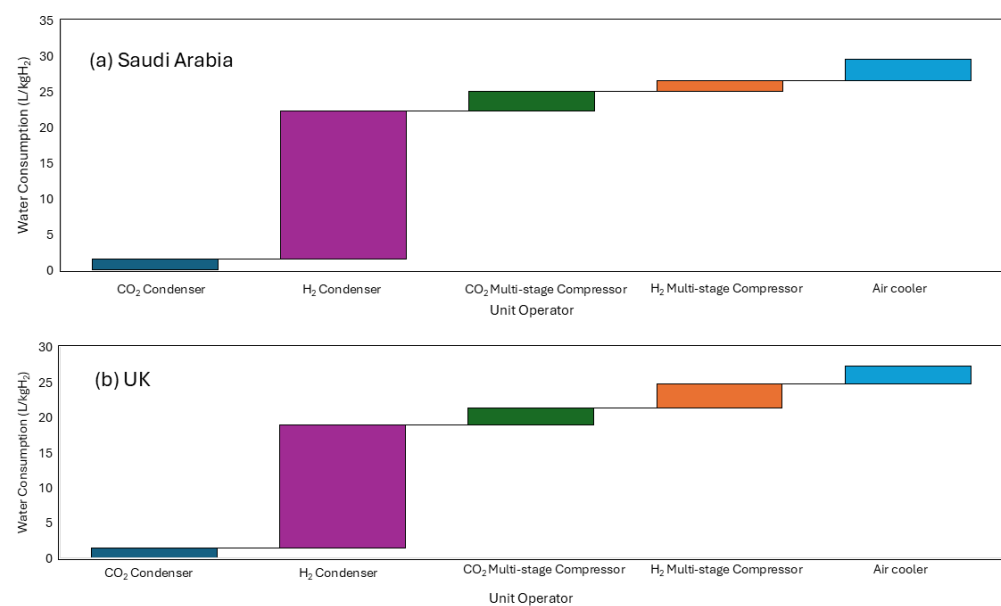


Figure 7. Breakdown of water consumption for each unit operator within the cooling.

3.3. Techno-Economic Assessment

In each scenario, a breakdown of the LCOH is presented in Figure 8a–d, with Table 11 providing a breakdown of the costs within the system and the LCOH and COCA. Due to the higher costs associated with electricity, NG, and CO₂ storage, the LCOH for this process within the UK is significantly elevated, at ~GBP 2.94/kg H₂ for both air and water cooling. Within the UK, water cooling has a slightly higher TCR than air cooling. Despite the increased TCR for the air-cooling scenario and higher electricity costs within the VOM, there is no significant difference in cost. However, in the Saudi Arabia scenario, the impact of higher water costs (both process and cooling water) and lower natural gas and electricity costs results in the water-cooling scenario having a higher LCOH at GBP 0.72/kg H₂ compared to GBP 0.70/kg H₂ for air cooling. As shown in Figure 8 within the UK there is a significantly higher VOM and NG impact on the LCOH mostly due to the increased electricity and NG prices. Despite these additional costs, the LCOH is not as significantly different as these factors will impact grey hydrogen production as well.

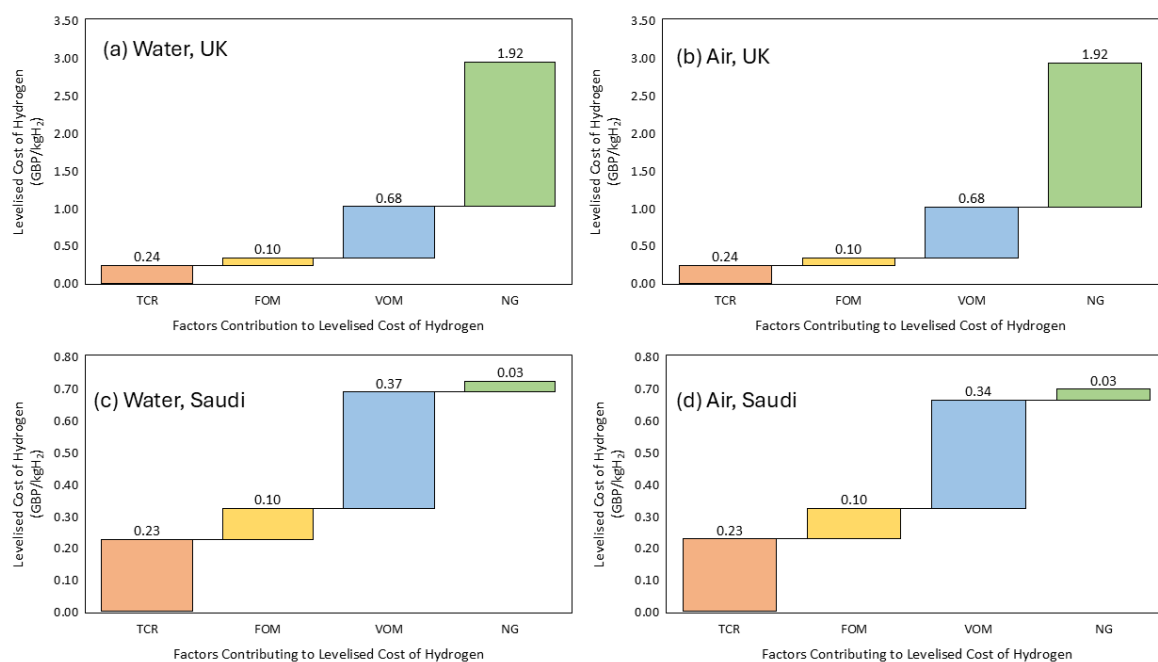


Figure 8. Breakdown of impact on TCR, FOM, VOM, and NG on (a) water cooling, UK, (b) air cooling, UK, (c) water cooling, Saudi Arabia, (d) air cooling, Saudi Arabia.

Table 11. TEA analysis of each scenario.

	Water, UK	Air, UK	Water, Saudi Arabia	Air, Saudi Arabia
TCR (GBP/million)	327.41	327.31	314.40	315.68
BEC (GBP/million)	185.01	184.95	185.07	185.86
FOM (GBP/million)	14.72	14.72	14.21	14.26
VOM (GBP/million)	100.62	99.62	52.88	50.01
NG price (GBP/kWh)	0.04	0.04	0.0007	0.0007
Net heat rate (kWh)	48.12	48.12	48.12	48.12
LCOH	2.94	2.94	0.70	0.72
LCOH (considering carbon emission tax for UK scenarios)	2.95	2.95	0.70	0.72
COCA (GBP/tonneCO ₂)	34.64	33.94	13.20	10.71

A breakdown of the BEC is illustrated in Figure 9. The majority of the BEC derives from the sorbent-enhanced reformer, calciner, CLC reactors, and the PSA unit. The heat exchangers and coolers make up a small portion of the TCR; therefore, while air cooling will incur a higher TCR for the Saudi Arabia scenario, it has a lesser impact on the overall LCOH. The technological uncertainty of the CLC and sorption-enhanced reformer were considered within this.

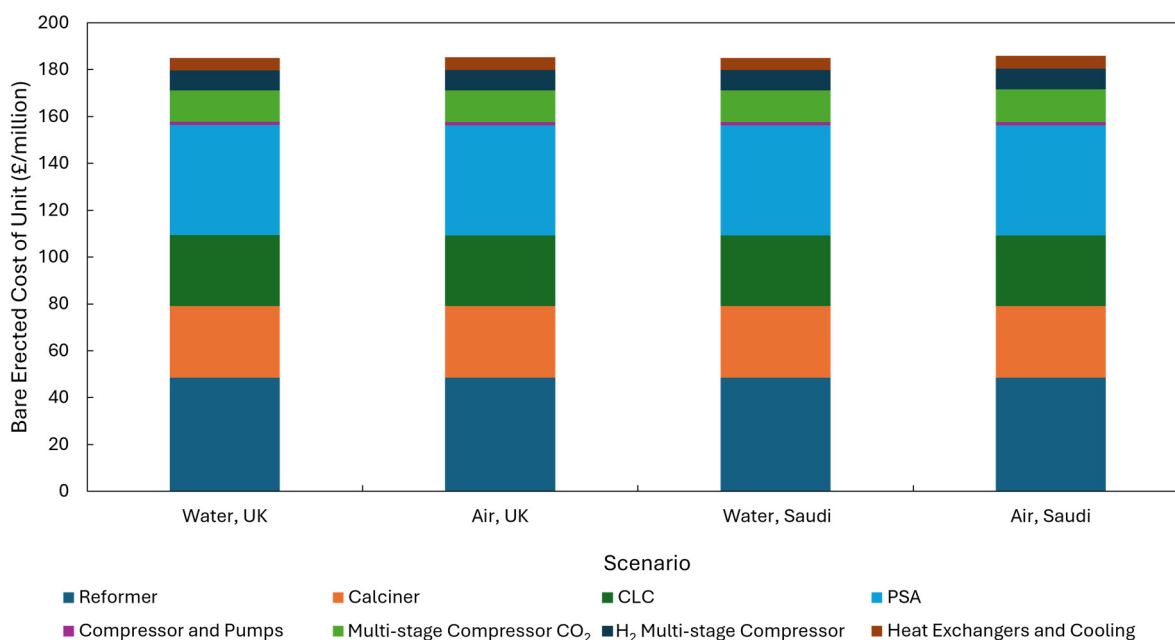


Figure 9. Breakdown of BEC across each scenario.

A further breakdown of the VOM is provided in Figure 10. As shown in Figure 10, due to the lower electricity prices in Saudi Arabia, the VOM is significantly reduced, with the costs of process water and CO₂ storage and transportation becoming the main factors affecting the LCOH in the Saudi Arabia scenarios. Across the scenarios, it is clear that air cooling is the slightly cheaper approach as despite the increased electrical consumption from the air cooling it is still cheaper for air-cooling scenarios due to the cooling water price which impacts particular in arid regions like Saudi Arabia. Often within the literature, air cooling is an expensive method due to the increased TCR costs associated with larger heat exchanger sizes as well as the electricity consumption associated with the fan power for each air-based heat exchanger; however, the TCR for the cooling tower, as well as electricity consumption for the mechanical forced draft cooling tower by the fan, mean that the increased costs associated with air cooling is not as significant.

In the UK, the greatest impact on the LCOH (accounting for GBP 1.92/kg H₂) is the natural gas price at GBP 0.04/kWh, which has risen significantly over the last few years due to various global factors. These include the Russia–Ukraine war, which has reduced supply, especially in Europe, and increased demand from Asian and South American markets as they shift away from coal [42,43]. This combination of reduced supply and heightened demand has posed challenges for the UK, given its reliance on natural gas imports from abroad [42]. This increase in the NG price subsequently affects electricity costs, with the wholesale price of electricity also rising, as shown in Figure 11. The volatility of NG pricing due to this current political and economic climate does mean countries that are reliant on NG imports (such as the UK) for electricity generation will be significantly impacted by variations in NG prices. This will be further discussed in Section 4.

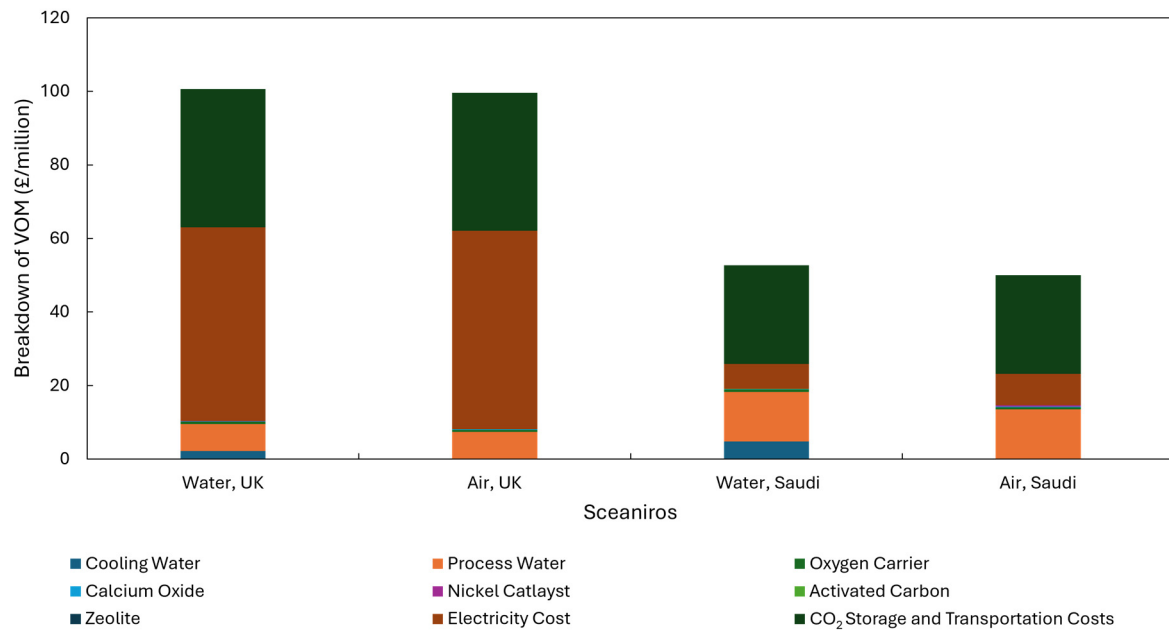


Figure 10. Breakdown of VOM across each scenario.

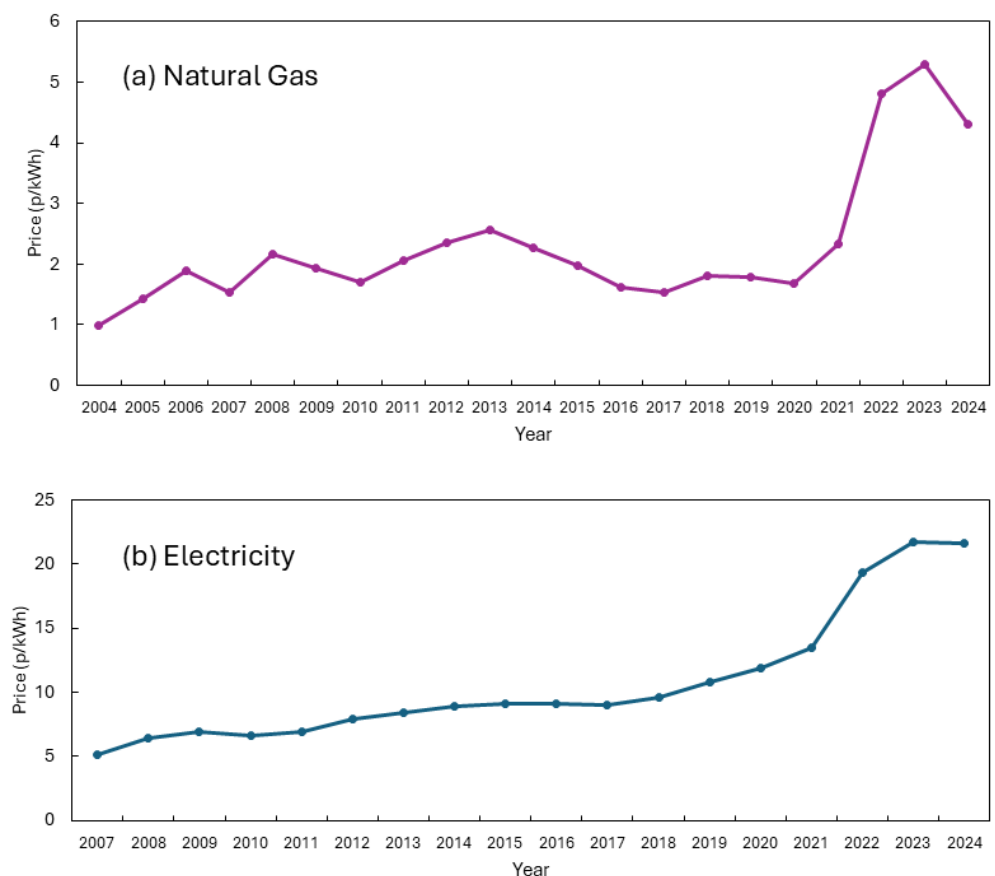


Figure 11. Yearly wholesale prices of UK (a) natural gas, (b) electricity.

Due to the variation in methods and assumptions (as well as recent volatility within NG prices), when calculating the LCOH, it can be challenging. However, based on recent literature, the SE-SMR-CLC process is cheaper in cost with conventional blue hydrogen production methods, which is in line with the general trend in the literature [20,30,44,45]. For example, Udemu et al. (2023) recently evaluated different blue hydrogen production processes and found that SE-SMR had a LCOH of GBP 2.84/kg H₂, significantly lower than

a SMR unit with amine scrubber LCOH at GBP 3.48/kg H₂ [44]. Considering Saudi Arabia recent work has evaluated different hydrogen production technologies within Saudi Arabia, Al-Khelaiwi et al. (2024) evaluated the LCOH of blue and green hydrogen production routes and determined that blue hydrogen with conventional CCS (amine scrubbing) achieved a LCOH of GBP 0.71/kg H₂ [30].

3.3.1. Sensitivity Analysis of Prices

Across the scenarios within the VOM, prices will differ, necessitating a sensitivity analysis to evaluate the impact of NG, electricity, CO₂ storage and transportation, and process water prices on the LCOH and COCA. The hydrogen production capacity and capacity factors were also assessed for the LCOH. Table 12 offers an overview of the values considered, which are location dependent. The reference grey hydrogen production prices used to calculate the COCA are GBP 2.60 and GBP 0.59/kg H₂ for the UK and Saudi Arabia, respectively [30,44]. As the COCA is calculated without considering any emission tax, it effectively represents the minimum emission tax required for this production route to remain competitive with higher-emission hydrogen production routes.

Table 12. Prices considered within each scenario for sensitivity analysis.

Pricing	Scenarios			
	UK		Saudi Arabia	
Electricity prices (GBP/kWh)	Lower bound	0.1	Lower bound	0.01
	Upper bound	0.3	Upper bound	0.1
	Difference	0.05	Difference	0.01
Natural gas prices (GBP/kWh)	Lower bound	0.01	Lower bound	0.0005
	Upper bound	0.08	Upper bound	0.0023
	Difference	0.01	Difference	0.0002
Process water prices (GBP/m ³)	Lower bound	2	Lower bound	4
	Upper bound	5	Upper bound	6
	Difference	0.50	Difference	0.50
CO ₂ storage and transportation costs prices (GBP/tonneCO ₂)	Lower bound	10	Lower bound	10
	Upper bound	40	Upper bound	40
	Difference	5	Difference	5
Hydrogen production capacity (MW)	Lower bound	50	Lower bound	50
	Upper bound	600	Upper bound	600
	Difference	275	Difference	275
Capacity factor (MW)	Lower bound	500	Lower bound	500
	Upper bound	600	Upper bound	600
	Difference	25	Difference	25

Natural Gas Prices

Figure 12a–d illustrates the impact of natural gas prices across all scenarios in the UK and Saudi Arabia. Within the UK, natural gas exerts the most significant effect on the LCOH and COCA, whereas in Saudi Arabia, its influence is less pronounced. Within the UK, should natural gas prices rise by GBP 0.02/kWh, the LCOH would increase by GBP 1/kg H₂, with the COCA also climbing by GBP 100/tonneCO₂. Although the sensitivity analysis does not consider the impact of the NG price on grey hydrogen production, this

will subsequently affect the LCOH of the steam-methane reforming process and, in turn, influence the COCA.

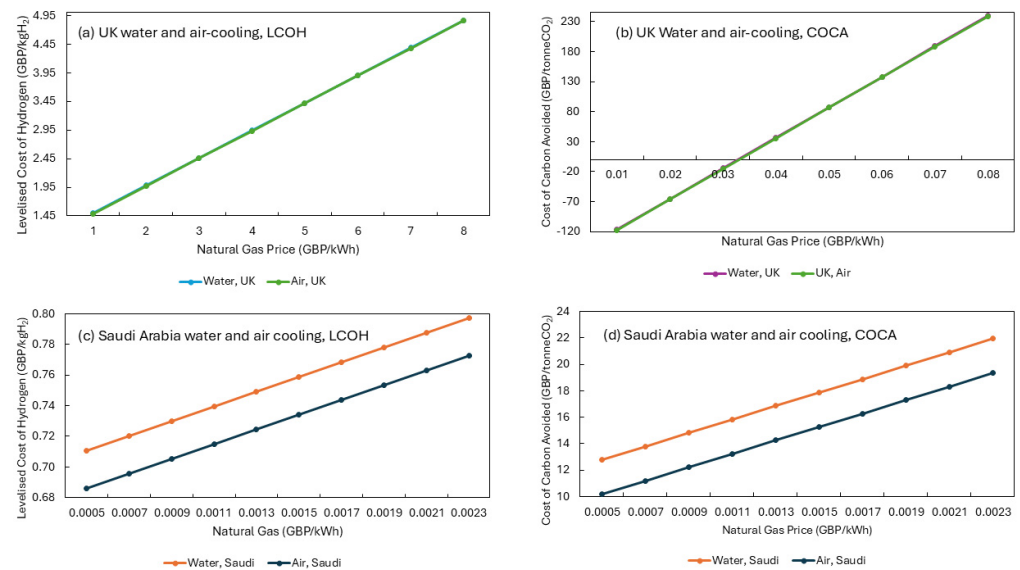


Figure 12. Sensitivity analysis of natural gas prices on LCOH and COCA. (a) UK water and air cooling, LCOH. (b) UK water and air cooling, COCA. (c) Saudi Arabia water and air cooling, LCOH. (d) Saudi Arabia water and air cooling, COCA.

Electricity Prices

Due to variations in electricity consumption across different scenarios, those that utilise air-cooling appear to be slightly more affected by electricity costs due to the higher consumption rates associated with air-cooling in both countries. As shown in Figure 13a–d, when electricity costs are elevated, the air cooling LCOH and COCA increase at a greater rate. In the UK, when the electricity price is lower, the LCOH for the air-cooling scenario is reduced, owing to the additional utility costs of cooling water in the water-cooling scenario. However, as electricity prices rise, the LCOH becomes the same across both scenarios. In Saudi Arabia, a similar trend is observed; however, due to the lower cost of electricity in the region, the air-cooling scenarios remain the more economical option for LCOH.

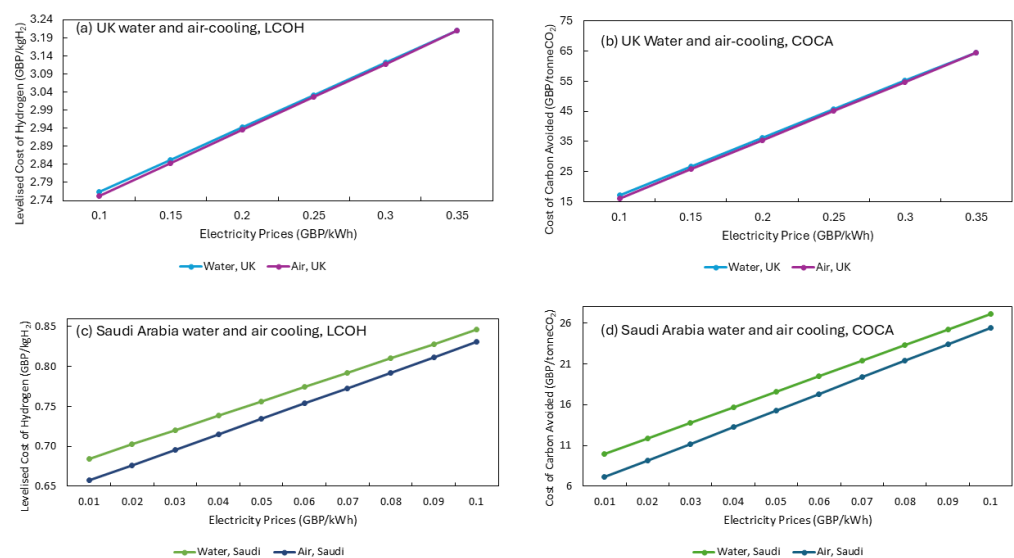


Figure 13. Sensitivity analysis of electricity prices on LCOH and COCA. (a) UK water and air cooling, LCOH. (b) UK water and air cooling, COCA. (c) Saudi Arabia water and air cooling, LCOH. (d) Saudi Arabia water and air cooling, COCA.

Process Water Prices

Variation of the process water yields a smaller impact on the LCOH and the COCA, as shown in Figure 14, which in comparison to NG prices and electricity prices is due to the impact of the process water on the VOC. Across both countries, air cooling is the cost-effective choice, despite the increased CAPEX considerations.

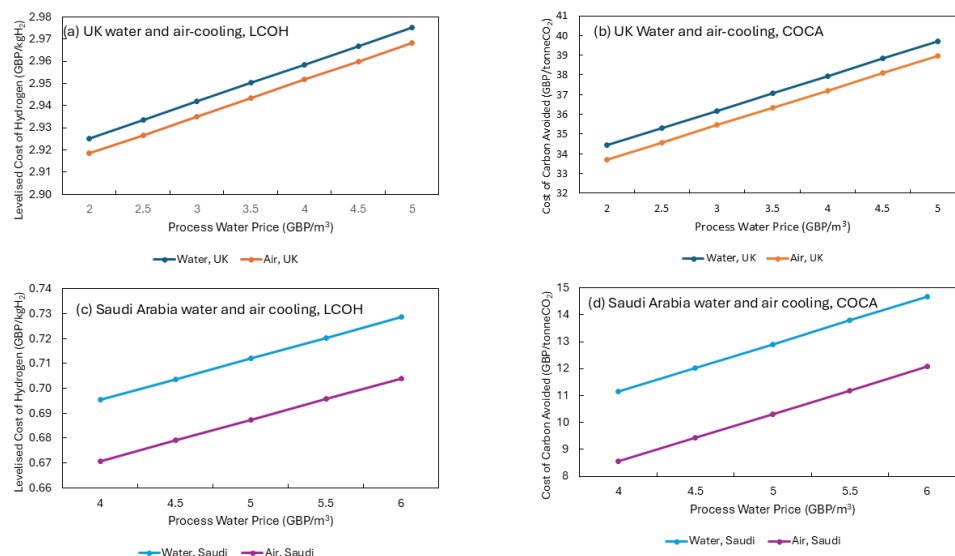


Figure 14. Sensitivity analysis of process water prices on LCOH and COCA. (a) UK water and air cooling, LCOH. (b) UK water and air cooling, COCA. (c) Saudi Arabia water and air cooling, LCOH. (d) Saudi Arabia water and air cooling, COCA.

CO₂ Storage and Transportation Prices

The CO₂ storage and transportation costs on large-scale plants such as this process are key due to the large amount of CO₂ captured. As shown in Figure 15a–d, minimising these costs is key to ensure that blue hydrogen is competitive with grey hydrogen production technologies. If these costs are minimised within the Saudi Arabia region, due to the low electricity and NG prices, it can be competitive with grey hydrogen production processes, needing only a carbon tax of GBP 6/tonneCO₂.

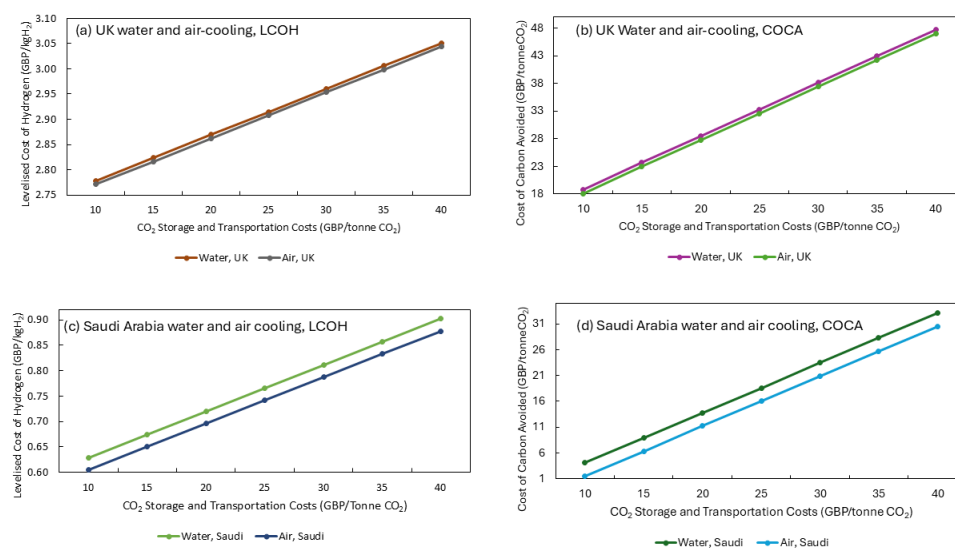


Figure 15. Sensitivity analysis of CO₂ storage and transportation prices on LCOH and COCA. (a) UK water and air cooling scenarios, LCOH. (b) UK water and air cooling, COCA. (c) Saudi Arabia water and air cooling, LCOH. (d) Saudi Arabia water and air cooling, COCA.

3.3.2. Hydrogen Production Capacity and Capacity Factor

The hydrogen production capacity was varied from 50 MW to 600 MW (with changes to BEC) to assess the variation in the LCOH. This is shown in the sensitivity analysis plots in Figure 16a,b for each scenario. The trends in Figure 16a,b indicate that increasing the production capacity reduces the LCOH in all scenarios, demonstrating how economies of scale may operate. A larger hydrogen production capacity means fixed costs, such as FOCs, are spread over a greater amount of hydrogen produced, lowering the overall cost. The capacity factor was included for the 600 MW plant, where the capacity was reduced to a minimum of 500 MW, whilst maintaining the same equipment size. The impact of this variation on the LCOH is shown in Figure 16c,d. Ensuring the plant operates at full capacity in each scenario is important for keeping the LCOH low (GBP 2.94/kg H₂ and 0.70–GBP 0.72/kg H₂ for Saudi Arabia), especially within the UK, where even reducing the capacity of a 600 MW plant to 500 MW results in an LCOH of GBP 3.60/kg H₂, comparable to a hydrogen production facility of 50 MW with an LCOH of GBP 3.67/kg H₂. This is most likely due to the increased VOC costs in the UK compared to Saudi Arabia. This, as shown in Figure 16d, has a less pronounced impact on the LCOH when reducing the capacity of the H₂ production facility to 500 MW.

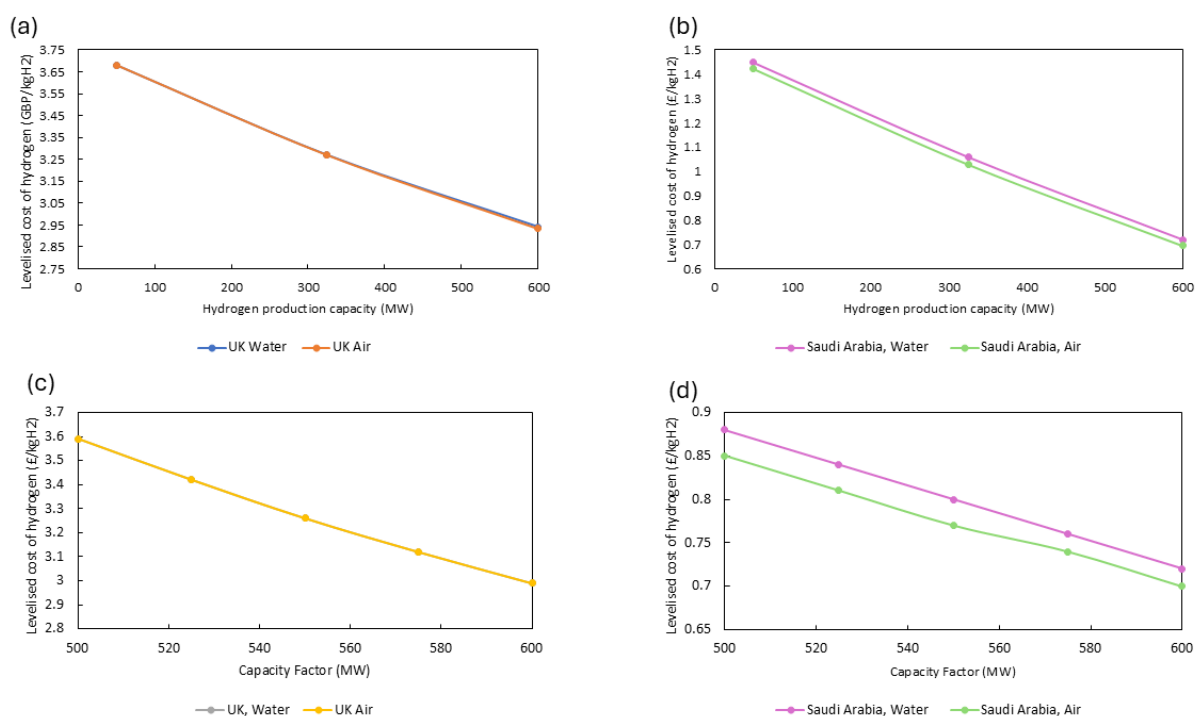


Figure 16. Sensitivity analysis plots for hydrogen production capacity and capacity factor. (a) UK hydrogen production capacity. (b) Saudi Arabia hydrogen production capacity. (c) UK capacity factor. (d) Saudi Arabia capacity factor.

3.3.3. Ranking the Impacts of the Variables Within the Sensitivity Analysis

In order to determine the impact of each factor on the LCOH, a tornado plot was developed for each scenario and is shown in Figure 17a–d. What is noticeable within Figure 17, is the regional variation in these factors that impact the LCOH. For example, NG price is the most significant factor for the LCOH within the UK. Increasing the NG prices to GBP 0.1/kWh increases the LCOH of the process to GBP 4.87/kg H₂, whereas in Saudi Arabia, due to the increased availability of NG, the LCOH is not impacted as much. Across both UK scenarios (Figure 17a,b), production capacity and capacity factor are influential, with both showing that a reduction will increase the LCOH to ~GBP 3.60/kg H₂.

For Saudi Arabia, the biggest driving factor is the hydrogen production capacity, showing that reducing the hydrogen production capacity of 50 MW, increases the LCOH to GBP 1.44–1.42/kg H₂. For both countries, a sustainable demand for the hydrogen is important to ensure there is a need for large-scale hydrogen production facilities that can operate at full capacity to keep LCOH low.

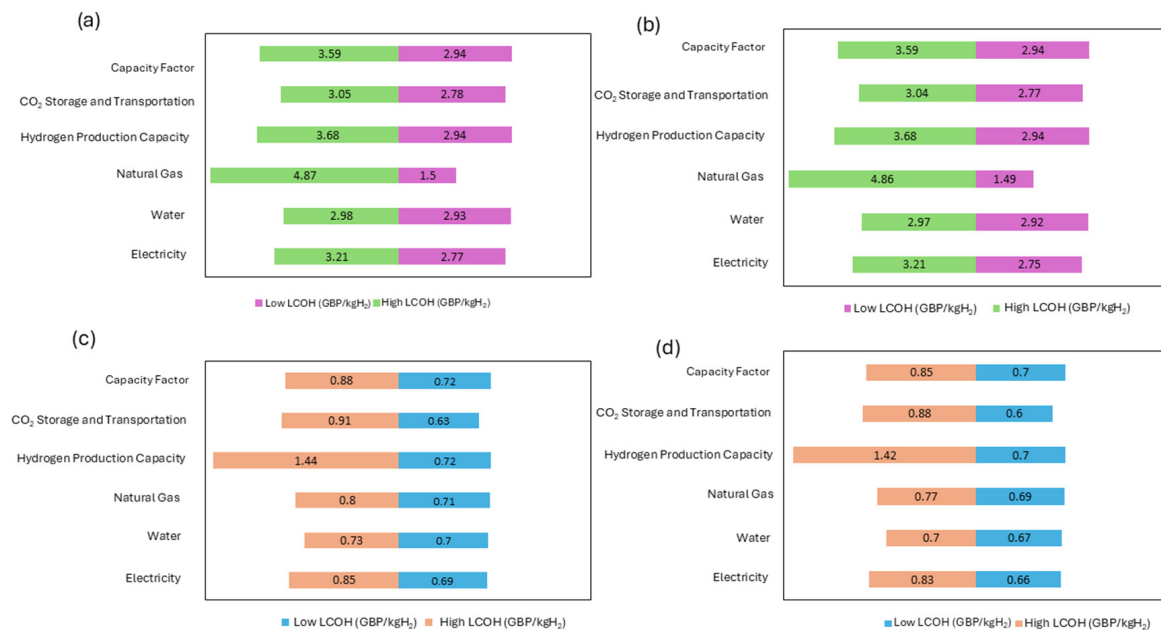


Figure 17. Tornado plots for: (a) UK, water. (b) UK, air. (c) Saudi Arabia, water. (d) Saudi Arabia, air.

4. Policy Implications: How to Incentivise Blue Hydrogen Production Effectively

Blue hydrogen has emerged as a critical transitional fuel in the global shift towards low-carbon energy systems. While technological advancements have significantly improved efficiency and reduced costs, effective policy mechanisms are required to accelerate large-scale deployment. Governments must focus on targeted incentives that address economic viability, infrastructure development, and sustainable cooling requirements to ensure widespread adoption. One of the most effective ways to promote blue hydrogen production is through direct financial incentives. Governments can implement subsidies that reduce the LCOH, making it competitive with conventional fuels [46]. For example, in regions such as the United Kingdom, where the LCOH is relatively high at GBP 2.94/kg H₂, subsidies can be structured to offset production costs, ensuring blue hydrogen remains a viable alternative. Tax credits and grants for industries investing in blue hydrogen infrastructure can further drive adoption. In Saudi Arabia, where the cost is significantly lower (around GBP 0.70–0.72/kg H₂), incentives could focus on supporting infrastructure and scaling up production to meet growing energy demands [47].

Another method to incentivise low-carbon technologies is through carbon pricing mechanisms, including carbon taxes and cap-and-trade systems, which can create market conditions that favour blue hydrogen production [48]. By increasing the cost of carbon-intensive alternatives, industries will be incentivised to transition towards cleaner hydrogen solutions. Setting aggressive emission reduction targets for heavy industries can further push investments in blue hydrogen technologies such as SE-SMR-CLC. Ethical considerations in carbon pricing frameworks are essential in guiding responsible corporate behaviour, particularly in emissions reduction [49]. In the UK, the COCA determined within Section 3.3.1 shows that a carbon tax of ~GBP 30/tonne CO₂ is needed to ensure it

is cost competitive with grey hydrogen production routes. Both processes are impacted by the NG costs, meaning that policy should incentivise reducing emissions within the process. The carbon tax can provide an approach to incentive capturing CO₂.

Scaling blue hydrogen production requires robust infrastructure, including storage, transport, and distribution networks. Governments can play a pivotal role by investing in hydrogen transport corridors, supporting pipeline development, and integrating hydrogen refuelling stations into existing energy grids. In geographically diverse regions, policies should address local energy requirements by optimising cooling methods. For instance, in arid environments such as Saudi Arabia, air cooling has proven viable method within minimal impact on the LCOH (GBP 0.70/kg H₂), despite its higher electricity consumption [50]. Policies should support energy-efficient cooling methods through research grants and technology development incentives. Based on the analysis, H₂ production capacity significantly impacts the LCOH for both the UK and Saudi Arabia. Developing large-scale production facilities ensures a lower LCOH: GBP 2.94/kg H₂ for the UK and GBP 0.70–0.72/kg H₂ for Saudi Arabia. Ensuring a market demand for hydrogen is vital. This demand must coincide with developing hydrogen infrastructure. In the UK, this development is particularly slow. For example, only 16 refuelling stations exist within the UK, which is significantly fewer than the 92 refuelling stations in Germany [51,52]. This adoption of hydrogen infrastructure is vital as the hydrogen produced should be linked to a sustainable end use, and without it, the large-scale production capacities are mostly redundant, leading to increased LCOH.

Furthermore, robust infrastructure is required for the storage and transportation of CO₂. As shown in this work, transportation and storage costs significantly impact the LCOH and COCA; in the UK, high CO₂ transportation and storage costs can increase the LCOH to GBP 3.05/tonneCO₂. Developing the infrastructure to ensure low transportation and storage costs is vital for the adoption of blue hydrogen. Similarly to hydrogen infrastructure, the surrounding infrastructure for CO₂ transportation and storage is key to ensure lower costs. As outlined by Brownsort et al. (2016), an approach to reducing the CAPEX costs is via sharing of pipelines within industrial clusters [53]. This development of industrial clusters is a key UK policy for industrial decarbonisation with two currently under development (HyNet and Humber) [54]. This policy allows for shared costs of CO₂ transportation and storage.

Governments should prioritise funding for research and development of advanced hydrogen technologies. This includes improving process efficiency, reducing reliance on energy-intensive cooling methods, and integrating CCS solutions. Academic institutions and private-sector partnerships should be encouraged through targeted grants, fostering innovation that enhances hydrogen production viability [55]. Studies indicate that investments in sustainability-focused technological advancements have a positive impact on financial markets and industry adoption [56]. In Saudi Arabia, the use of water-cooling approaches shows an increased LCOH at GBP 0.72/kg H₂, due to the increased costs of water in the region. The development of hybrid cooling approaches should focus on improving the energy efficiency of air-cooling processes and how this could further reduce LCOH [57].

Given the disparity in hydrogen production costs between regions, international collaboration is essential. Trade agreements can facilitate cross-border hydrogen exports, ensuring regions with lower production costs, such as Saudi Arabia, can supply countries with higher costs. Cooperative efforts in regulatory standards, shared infrastructure development, and policy harmonisation can further streamline the global hydrogen supply chain [50,58]. To effectively incentivise blue hydrogen production, policymakers must adopt a multifaceted approach. By implementing financial incentives, carbon pricing strategies, infrastructure support, research funding, and international collaboration, governments

can create favourable conditions for large-scale adoption. Tailoring policies to regional economic and environmental realities will ensure a balanced and sustainable transition towards clean hydrogen energy.

5. Conclusions

The SE-SMR-CLC process has been found to be a potentially competitive route for blue hydrogen production in both the UK and Saudi Arabia, with levelised costs of hydrogen (LCOH) estimated at approximately GBP 2.94/kg H₂ and GBP 0.70/kg H₂, respectively. Cooling method selection has a notable impact on process economics. In regions like Saudi Arabia, where water is a more expensive commodity, air cooling offers a more cost-effective option. Specifically, water cooling results in an LCOH of GBP 0.72/kg H₂, just slightly GBP 0.02/kg H₂ more than air cooling (GBP 0.70/kg H₂). This is despite the higher electrical consumption associated with air-cooling. However, the use of mechanical forced-draft cooling towers also contributes significantly to electricity demand in water-cooling scenarios. When combined with increased water usage, this makes air cooling the preferred option for blue hydrogen production in such regions. A key factor influencing cooling demand is the high steam-to-carbon (S/C) ratio employed. Although this ratio offers process advantages, it also increases the energy required for stream heating and cooling. Further analysis of operating conditions and inter-stream interactions is needed to fully assess the process's large-scale viability. Despite the SE-SMR-CLC system's high efficiency and strong CO₂ capture potential, widespread adoption will depend on supportive policy frameworks and financial incentives. Future work will explore how such mechanisms can be applied to accelerate deployment of this promising technology.

Supplementary Materials: The following supporting information can be downloaded at: <https://www.mdpi.com/article/10.3390/pr13082638/s1>. Figure S1: Process flowsheet of sorption-enhanced steam methane reforming with chemical-looping combustion. Table S1: Results of validation of sorption-enhanced reformer. Table S2: Stream table for UK water-cooling scenario. Table S3: Stream table for UK air-cooling scenario. Table S4: Stream table for Saudi Arabia water-cooling scenario. Table S5: Stream table for Saudi Arabia water-cooling scenario. Table S6: Sizing water-cooling heat exchangers for UK scenario. Table S7: Parameters for calculating area of heat exchangers for air-coolers in UK scenario. Table S8: Parameters for sizing heat exchanger for water cooling in Saudi Arabia scenario. Table S9: Parameters for sizing heat exchangers for air cooling in Saudi Arabia scenario. Table S10: Scaling parameters used for bare erected cost across all scenarios [7,21,59–65].

Author Contributions: Conceptualization, S.M.S. and W.G.D.; methodology, S.M.S., W.G.D., and S.B.; software, W.G.D.; validation, W.G.D. and I.G.; formal analysis, W.G.D., I.G., and S.B.; investigation, W.G.D., I.G., S.B., and M.G.; resources, S.M.S.; data curation, S.M.S.; writing—original draft preparation, W.G.D., S.B., M.G., and M.N.; writing—review and editing, S.M.S. and F.C.; visualization, S.M.S. and W.G.D.; supervision, S.M.S.; project administration, S.M.S.; funding acquisition, S.M.S. All authors have read and agreed to the published version of the manuscript.

Funding: The research presented in this work has received financial support from the UK Engineering and Physical Sciences Research Council (EPSRC) through the EPSRC Doctoral Training Partnerships (DTP) award, EP/T518116/1 (project reference: 2688399).

Data Availability Statement: Data have been made available in Brunel University of London's repository via the Brunel Figshare database at 10.17633/rd.brunel.29479115.

Conflicts of Interest: Author Francesco Coletti was employed by the company Hexxcell Ltd. The remaining authors declare that the research was conducted in the absence of any commercial or financial relationships that could be construed as a potential conflict of interest. The company Hexxcell Ltd. had no role in the design of the study; in the collection, analyses, or interpretation of data; in the writing of the manuscript, or in the decision to publish the results.

Nomenclature

Air reactor	AR
Air-separation unit	ASU
Bare erected costs	BEC
Capacity factor	CF
Carbon capture efficiency	CCE
Carbon capture storage	CCS
Chemical Engineering Plant Cost Index	CEPCI
Chemical-looping combustion	CLC
Cold gas efficiency	CGE
Cost of carbon avoided	COCA
Cycles of concentration	COC
Discount rate	r
Economic lifetime of plant	T
Engineering Procurement Construction Cost	EPCC
Fixed charge factor	FCF
Fixed operational costs	FOM
Fuel costs	FC
Fuel reactor	FR
Greenhouse gas	GHG
Heat exchanger network	HEN
International Renewable Energy Agency	IRENA
Levelised cost of hydrogen	LCOH
Lower heating value	LHV
Natural gas	NG
Net heat rate of plant	HR
Net process efficiency	NPE
Operational expenditure	OPEX
Pressure swing adsorption	PSA
Sorption-enhanced steam methane reforming	SE-SMR
Sorption-enhanced steam methane reforming with chemical-looping combustion	SE-SMR-CLC
Steam/carbon	S/C
Steam generator	SG
Steam methane reforming	SMR
Technology readiness level	TRL
Total capital requirement	TCR
Total electrical consumption	TEC
Total plant costs	TPC
Total process efficiency	TPE
Variable operational costs	VOM

References

1. Zhu, Y.; Keoleian, G.A.; Cooper, D.R. The role of hydrogen in decarbonizing U.S. industry: A review. *Renew. Sustain. Energy Rev.* **2025**, *214*, 115392. [[CrossRef](#)]
2. Babamohammadi, S.; Davies, W.G.; Soltani, S.M. Probing into the interactions among operating variables in blue hydrogen production: A new approach via design of experiments (DoE). *Gas Sci. Eng.* **2023**, *117*, 205071. [[CrossRef](#)]
3. Mostafa, A.; Beretta, A.; Groppi, G.; Tronconi, E.; Romano, M.C. A novel electrified sorption enhanced reforming process for blue hydrogen production. *Energy Adv.* **2025**, *4*, 624–638. [[CrossRef](#)]
4. Balasubramanian, B.; Ortiz, A.L.; Kaytakoglu, S.; Harrison, D.P. Hydrogen from methane in a single-step process. *Chem. Eng. Sci.* **1999**, *54*, 3543–3552. [[CrossRef](#)]
5. Soltani, S.M.; Lahiri, A.; Bahzad, H.; Clough, P.; Gorbounov, M.; Yan, Y. Sorption-enhanced Steam Methane Reforming for Combined CO₂ Capture and Hydrogen Production: A State-of-the-Art Review. *Carbon Capture Sci. Technol.* **2021**, *1*, 100003. [[CrossRef](#)]

6. Mays, J. One-Step Hydrogen Generation Through Sorption Enhanced Reforming. Available online: <https://www.osti.gov/servlets/purl/1373949/> (accessed on 25 May 2025).
7. Yan, Y.; Manovic, V.; Anthony, E.J.; Clough, P.T. Techno-economic analysis of low-carbon hydrogen production by sorption enhanced steam methane reforming (SE-SMR) processes. *Energy Convers. Manag.* **2020**, *226*, 113530. [CrossRef]
8. Spallina, V.; Shams, A.; Battistella, A.; Gallucci, F.; Annaland, M.V.S. Chemical Looping Technologies for H₂ Production with CO₂ Capture: Thermodynamic Assessment and Economic Comparison. *Energy Procedia* **2017**, *114*, 419–428. [CrossRef]
9. Martínez, I.; Romano, M.C.; Chiesa, P.; Grasa, G.; Murillo, R. Hydrogen production through sorption enhanced steam reforming of natural gas: Thermodynamic plant assessment. *Int. J. Hydrogen Energy* **2013**, *38*, 15180–15199. [CrossRef]
10. Yan, Y.; Thanganadar, D.; Clough, P.T.; Mukherjee, S.; Patchigolla, K.; Manovic, V.; Anthony, E.J. Process simulations of blue hydrogen production by upgraded sorption enhanced steam methane reforming (SE-SMR) processes. *Energy Convers. Manag.* **2020**, *222*, 113144. [CrossRef]
11. Phuluanglue, A.; Khaodee, W.; Assabumrungrat, S. Simulation of intensified process of sorption enhanced chemical-looping reforming of methane: Comparison with conventional processes. *Comput. Chem. Eng.* **2017**, *105*, 237–245. [CrossRef]
12. Alam, S.; Kumar, J.P.; Rani, K.Y.; Sumana, C. Self-sustained process scheme for high purity hydrogen production using sorption enhanced steam methane reforming coupled with chemical looping combustion. *J. Clean Prod.* **2017**, *162*, 687–701. [CrossRef]
13. Camacho, C.E.G.; Fernandez, E.B.; González-Delgado, Á.D.; Vargas-Mira, A.; Zuluaga-García, C. Economic Evaluation and Technoeconomic Resilience Analysis of Two Routes for Hydrogen Production via Indirect Gasification in North Colombia. *Sustainability* **2023**, *15*, 16371. [CrossRef]
14. D’Antoni, M.; Romeli, D.; Fedrizzi, R. *Techno-Economic Analysis of Air-to-Water Heat Rejection Systems*; ISES: Freiburg, Germany, 2015; pp. 1–8. [CrossRef]
15. Kumar, P.; Date, A.; Mahmood, N.; Das, R.K.; Shabani, B. Freshwater supply for hydrogen production: An underestimated challenge. *Int. J. Hydrogen Energy* **2024**, *78*, 202–217. [CrossRef]
16. Lin, N.; Arzumanyan, M.; Calzado, E.R.; Nicot, J.P. Water Requirements for Hydrogen Production: Assessing Future Demand and Impacts on Texas Water Resources. *Sustainability* **2025**, *17*, 385. [CrossRef]
17. The Energy Water Nexus: Balancing Water Needs for Hydrogen Production. 2023. Available online: <https://www.arup.com/insights/the-energy-water-nexus-balancing-water-needs-for-hydrogen-production> (accessed on 25 May 2025).
18. Ellersdorfer, P.; Omar, A.; Rider, I.; Daiyan, R.; Leslie, G. The hydrogen-water collision: Assessing water and cooling demands for large-scale green hydrogen production in a warming climate. *Int. J. Hydrogen Energy* **2025**, *97*, 1002–1013. [CrossRef]
19. International Renewable Energy Agency Water for Hydrogen Production. 2023. Available online: www.irena.org (accessed on 25 May 2025).
20. Eluwah, C.; Fennell, P.S.; Tighe, C.J.; Al Dawood, A. A novel technological blue hydrogen production process: Industrial sorption enhanced autothermal membrane (ISEAM). *Energy Adv.* **2023**, *2*, 1476–1494. [CrossRef]
21. Davies, W.G.; Babamohammadi, S.; Yan, Y.; Clough, P.T.; Soltani, S.M. Exergy analysis in intensification of sorption-enhanced steam methane reforming for clean hydrogen production: Comparative study and efficiency optimisation. *Carbon Capture Sci. Technol.* **2024**, *12*, 100202. [CrossRef]
22. Mathias, P.M.; Copeman, T.W. Extension of the Peng-Robinson equation of state to complex mixtures: Evaluation of the various forms of the local composition concept. *Fluid Phase Equilib.* **1983**, *13*, 91–108. [CrossRef]
23. Bhatia, A. PDHonline Course M320 (7 PDH) Cooling Towers-Made Easy Cooling Towers-Made Easy. Available online: www.PDHonline.com (accessed on 10 February 2025).
24. Toward a Common Method of Cost Estimation for CO₂ Capture and Storage at Fossil Fuel Power Plants. 2013. Available online: <http://www.epp.cmu.edu/people/faculty/rubin/> (accessed on 5 June 2025).
25. Wassie, S.A.; Gallucci, F.; Zaabout, A.; Cloete, S.; Amini, S.; van Sint Annaland, M. Hydrogen production with integrated CO₂ capture in a novel gas switching reforming reactor: Proof-of-concept. *Int. J. Hydrogen Energy* **2017**, *42*, 14367–14379. [CrossRef]
26. Quality Guidelines for Energy System Studies: Cost Estimation Methodology for NETL Assessments for Power Plant Performance. 2021. Available online: <https://www.osti.gov/biblio/1567736> (accessed on 25 May 2025).
27. Chemical Plant Process Operator. Available online: <https://nationalcareers.service.gov.uk/job-profiles/chemical-plant-process-operator> (accessed on 28 June 2025).
28. Chemical Plant Operator Saudi Arabia. Available online: <https://www.salaryexpert.com/salary/job/chemical-plant-operator/saudi-arabia> (accessed on 28 June 2025).
29. Gas and Electricity Prices in the Non-Domestic Sector—GOV.UK. Available online: <https://www.gov.uk/government/statistical-data-sets/gas-and-electricity-prices-in-the-non-domestic-sector> (accessed on 28 June 2025).
30. Al-Khelaiwi, M.S.; Al-Masaabi, T.A.; Farag, H.; Rehman, S. Evaluation of Green and Blue Hydrogen Production Potential in Saudi Arabia. *Energy Convers. Manag.* **2024**, *24*, 100742. [CrossRef]
31. Black, P. The Cost of Water in the Process Industry. *Process Industry Informer*. Available online: <https://www.processindustryinformer.com/process-industry-water-cost/> (accessed on 28 June 2025).

32. Mcilwaine, S.J.; Ouda, O.K.M.; Mcilwaine, S. Drivers and challenges to water tariff reform in Saudi Arabia Drivers and Challenges to Water Tariff Reform in Saudi Arabia Publication details. *Int. J. Water Res. Dev.* **2020**, *36*, 1014–1030. [CrossRef]
33. Iron Oxide Synthetic—Potclays. Available online: <https://www.potclays.co.uk/iron-oxide-synthetic> (accessed on 28 June 2025).
34. Industrial Grade Calcium Oxide Cao Factory Price Inorganic Oxide Calcium Oxide for Water Treatment Chemicals—Buy High Quality Low Price Calcium Oxide Cao Food Grade Calcium Oxide Powder and Block for Food Additive High Purity Quicklime Powder Calcium Oxide 200 Mesh Vietnam Bulk Exporting for Mining Water Treatment industrial Grade 99.99 Calcium Oxide Cao Quicklime Powder Calcium Oxide for Industrial Cas 1305-78-8 Product on Alibaba.com. Available online: https://www.alibaba.com/product-detail/Industrial-Grade-Calcium-Oxide-CaO-Factory_1601377056188.html?spm=a2700.7724857.0.0.5c9c7350SCT8x5 (accessed on 28 June 2025).
35. Nickel—Price—Chart—Historical Data—News. Available online: <https://tradingeconomics.com/commodity/nickel> (accessed on 28 June 2025).
36. Premium Grade Coconut Shell Activated Carbon 4×6 & 6×12 Mesh Size Granular Bet 1200 For Gold Draw For Petroleum Additives—Buy Granular Coconut Shell Activated Carbon to Draw Gold water Treatment Coconut Carbon Product on Alibaba.com. Available online: https://www.alibaba.com/product-detail/4x6-6x12-mesh-size-granular-coconut_1601038976376.html?spm=a2700.7724857.0.0.181b3320vt5NBE (accessed on 28 June 2025).
37. China Factory Price Sphere Zeolite 13× Molecular Sieve in Oxygen Generators. Available online: https://www.alibaba.com/product-detail/China-Factory-Price-Sphere-Zeolite-13x_60661914797.html?spm=a2700.7724857.0.0.318820afwSWiky (accessed on 28 June 2025).
38. GlobalPetrolPrices.com. Saudi Arabia Electricity Prices. 2024. Available online: https://www.globalpetrolprices.com/Saudi-Arabia/electricity_prices/ (accessed on 28 June 2025).
39. Smith, E.; Morris, J.; Khesghi, H.; Teletzke, G.; Herzog, H.; Paltsev, S. The cost of CO₂ transport and storage in global integrated assessment modeling. *Int. J. Greenh. Gas Control* **2021**, *109*, 103367. [CrossRef]
40. Carbon Emissions Tax—GOV.UK. Available online: <https://www.gov.uk/government/publications/carbon-emissions-tax/carbon-emissions-tax> (accessed on 28 June 2025).
41. Brandl, P.; Soltani, S.M.; Fennell, P.S.; Dowell, N.M. Evaluation of cooling requirements of post-combustion CO₂ capture applied to coal-fired power plants. *Chem. Eng. Res. Des.* **2017**, *122*, 1–10. [CrossRef]
42. Factcheck: Why Expensive Gas—Not Net-Zero—Is Keeping UK Electricity Prices so High, Carbon Brief. Available online: <https://www.carbonbrief.org/factcheck-why-expensive-gas-not-net-zero-is-keeping-uk-electricity-prices-so-high/> (accessed on 28 June 2025).
43. Jackman, J. The 6 Key Reasons Behind the UK’s Gas Price Increases, eco experts. Available online: <https://www.theecoexperts.co.uk/news/reasons-for-uk-gas-price-increase> (accessed on 28 June 2025).
44. Udemu, C.; Font-Palma, C. Modelling of sorption-enhanced steam reforming (SE-SR) process in fluidised bed reactors for low-carbon hydrogen production: A review. *Fuel* **2023**, *340*, 127588. [CrossRef]
45. Nazir, S.M.; Cloete, J.H.; Cloete, S.; Amini, S. Pathways to low-cost clean hydrogen production with gas switching reforming. *Int. J. Hydrogen Energy* **2021**, *46*, 20142–20158. [CrossRef]
46. Nyangon, J.; Darekar, A. Advancements in hydrogen energy systems: A review of leveled costs, financial incentives and technological innovations. *Innov. Green Dev.* **2024**, *3*, 100149. [CrossRef]
47. Shabaneh, R.; Roychoudhury, J.; Braun, J.F.; Saxena, S. The clean hydrogen economy and Saudi Arabia: Domestic developments and international opportunities. In *The Clean Hydrogen Economy and Saudi Arabia: Domestic Developments and International Opportunities*; Taylor & Francis: New York, NY, USA, 2024; pp. 1–768. [CrossRef]
48. George, J.F.; Müller, V.P.; Winkler, J.; Ragwitz, M. Is blue hydrogen a bridging technology?—The limits of a CO₂ price and the role of state-induced price components for green hydrogen production in Germany. *Energy Policy* **2022**, *167*, 113072. [CrossRef]
49. Magnetti, J.; Dominion, G.; Gordijn, B. Ethics of carbon pricing—a review of the literature. *Climate Policy* **2024**, *25*, 772–791. [CrossRef]
50. Noussan, M.; Raimondi, P.P.; Scita, R.; Hafner, M. The Role of Green and Blue Hydrogen in the Energy Transition—A Technological and Geopolitical Perspective. *Sustainability* **2021**, *13*, 298. [CrossRef]
51. Uncertain Future: Hydrogen Fuel Stations UK—What’s Next? Available online: <https://pulseenergy.io/blog/hydrogen-fuel-stations-uk> (accessed on 1 July 2025).
52. VDA. Hydrogen and Tanking Infrastructure. Available online: <https://www.vda.de/en/topics/automotive-industry/commercial-vehicles/hydrogen-tanking-infrastructure> (accessed on 1 July 2025).
53. Brownsort, P.A.; Scott, V.; Haszeldine, R.S. Reducing costs of carbon capture and storage by shared reuse of existing pipeline—Case study of a CO₂ capture cluster for industry and power in Scotland. *Int. J. Greenh. Gas Control* **2016**, *52*, 130–138. [CrossRef]
54. D. for Energy Security and N. Zero CCUS Net Zero Investment Roadmap Capturing Carbon and a Global Opportunity. 2023. Available online: <https://www.gov.uk/government/publications/carbon-capture-usage-and-storage-net-zero-investment-roadmap/ccus-net-zero-investment-roadmap-capturing-carbon-and-a-global-opportunity> (accessed on 1 July 2025).

55. Wu, W.; Zhai, H.; Holubnyak, E. Technological evolution of large-scale blue hydrogen production toward the U.S. Hydrogen Energy Earthshot. *Nat. Commun.* **2024**, *15*, 5684. [CrossRef]
56. Allam, Z.; Cheshmehzangi, A. Sustainable Futures and Green New Deals. In *Sustainable Futures and Green New Deals*; Springer: Berlin/Heidelberg, Germany, 2024. [CrossRef]
57. Hybrid Wet Dry Cooling Tower with High Efficient & Energy Saving. Available online: <https://www.flycoolingtower.com/products/hybrid-wet-dry-cooling-tower/index.html> (accessed on 1 July 2025).
58. Cloete, S.; Ruhnau, O.; Cloete, J.H.; Hirth, L. Blue hydrogen and industrial base products: The future of fossil fuel exporters in a net-zero world. *J. Clean. Prod.* **2022**, *363*, 132347. [CrossRef]
59. García, R.; Gil, M.V.; Rubiera, F.; Chen, D.; Pevida, C. Renewable hydrogen production from biogas by sorption enhanced steam reforming (SESR): A parametric study. *Energy* **2020**, *218*, 119491. [CrossRef]
60. Johnsen, K.; Ryu, H.J.; Grace, J.R.; Lim, C.J. Sorption-enhanced steam reforming of methane in a fluidized bed reactor with dolomite as CO₂-acceptor. *Chem. Eng. Sci.* **2006**, *61*, 1195–1202. [CrossRef]
61. Rosner, F.; Chen, Q.; Rao, A.; Samuelsen, S. Thermo-economic analyses of isothermal water gas shift reactor integrations into IGCC power plant. *Appl. Energy* **2020**, *277*, 115500. [CrossRef]
62. Rath, L.K.; Chou, V.H.; Kuehn, N.J. Assessment of Hydrogen Production with CO₂ Capture Volume 1: Baseline State-of-the-Art Plants (Final Report). November 2011. Available online: <https://www.osti.gov/servlets/purl/1767148> (accessed on 1 July 2025).
63. Poto, S.; Vink, T.; Oliver, P.; Gallucci, F.; D'angelo, M.F.N. Techno-economic assessment of the one-step CO₂ conversion to dimethyl ether in a membrane-assisted process. *J. CO₂ Util.* **2023**, *69*, 102419. [CrossRef]
64. Manzolini, G.; Macchi, E.; Gazzani, M. CO₂ capture in natural gas combined cycle with SEWGS. Part B: Economic assessment. *Int. J. Greenh. Gas Control.* **2013**, *12*, 502–509. [CrossRef]
65. Parsons, E.; Shelton, W.; Lyons, J.L. Advanced Fossil Power Systems Comparison Study. 2002. Available online: <https://citeseerx.ist.psu.edu/document?repid=rep1&type=pdf&doi=bdbee1effd3f63bb04dc468eef3dfff0699782d2f> (accessed on 28 June 2025).

Disclaimer/Publisher's Note: The statements, opinions and data contained in all publications are solely those of the individual author(s) and contributor(s) and not of MDPI and/or the editor(s). MDPI and/or the editor(s) disclaim responsibility for any injury to people or property resulting from any ideas, methods, instructions or products referred to in the content.